Age and Learning Shapes Sound Representations in Auditory Cortex During Adolescence

Praegel Benedikt[1,2], Chen Feng[3,4], Dym Adria[1], Lavi-Rudel Amichai[1], Druckmann Shaul[3,5], and Mizrahi Adi[1,2,*]

[1]The Edmond and Lily Safra Center for Brain Sciences. [2]Department of Neurobiology, the Institute of Life Sciences. The Hebrew University of Jerusalem, Jerusalem, Israel. [3]Department of Neurobiology, Stanford University, Stanford, California, USA. [4]Department of Applied Physics, Stanford University, Stanford, California, USA. [5]Department of Psychiatry and Behavioral Sciences, Stanford University, Stanford, California, USA.

** Corresponding author: Adi Mizrahi: Mizrahi.adi@mail.huji.ac.il*

Summary

Adolescence is a developmental period characterized by heightened plasticity, yet how ongoing development affects sensory processing and cognitive function is unclear. We investigated how adolescent (postnatal day 40 ± 2) and adult (postnatal day 80 ± 2) mice differ in performance on a pure tone Go/NoGo auditory discrimination task of varying difficulty. Using dense electrophysiological recordings, we measured spiking activity at single neuron resolution in the auditory cortex while mice were engaged in the task. Adolescent mice showed lower auditory discrimination performance compared to adults, particularly in more challenging versions of the discrimination. This performance difference was due to higher response variability and weaker cognitive control expressed as lower response bias. Adolescent and adult neuronal responses differed only slightly in representations of pure tones when measured outside the context of learning and the task. However, cortical representations after learning within the context of the task were markedly different. We found differences in stimulus- and choice-related activity at the single neuron level representations, as well as lower population-level decoding in adolescents. Overall, cortical decoding in adolescents was lower and slower, especially for difficult sound discrimination, reflecting immature cortical representations of sounds and choices. Notably, we found age-related differences, which were higher after learning, reflecting the combined impact of age and learning. Our findings highlight distinct neurophysiological and behavioral profiles in adolescence, underscoring the ongoing development of cognitive control mechanisms and cortical plasticity during this sensitive developmental period.

Keywords:
Adolescence, Auditory Cortex, Auditory Learning, Neuropixels, Neuronal Coding

Introduction

Adolescence is a developmental stage characterized by the continued refinement of perception and cognition. During this period, the brain is highly sensitive to environmental influences, making it particularly vulnerable to both negative experiences, such as substance abuse, and positive influences, such as supportive relationships(*1, 2*). While the adolescent brain exhibits greater plasticity compared to adults(*3*), the extent to which specific sensory and cognitive traits are fully developed versus those that remain malleable is still debated. For instance, studies on sensory perception have demonstrated that adolescent learning is slower and more variable(*4, 5*), while others have found that adolescents learn faster in novel contexts, such as reversal learning(*6*). Certain traits, such as cognitive flexibility, are more pronounced in adolescents compared to adults, whereas other behaviors such as impulsive control, are still immature(*7*). Furthermore, results across studies that target sensory or cognitive traits are often inconsistent(*8*). Therefore, understanding the degree to which sensory and cognitive functions have matured and the underlying brain mechanisms that support them remain an ongoing challenge.

A key concept in brain development is that of critical periods (CPs), which are specific time windows during which the brain's neural circuits are highly plastic and particularly sensitive to external experiences(*9, 10*). The early postnatal development of sensory cortices provides classical examples of this phenomenon. In mice, neurons in the visual cortex undergo several CP's such as those for orientation selectivity, direction selectivity and ocular dominance. During the CP, which occurs in different developmental time windows for different functional attributes, visual experience shapes the specific neuronal attribute to a long-term state (e.g., ocular dominance reaches its adult form)(*9, 11*). The CPs for simple neuronal features in primary sensory cortices are typically complete by the onset of puberty. In the auditory cortex (ACx) of mice the CP for pure tone processing begins as early as postnatal day 12 (P12), shortly after the ear canals open, and closes by ~P15(*12-15*). Thus, the closure of the auditory CP to pure tones occurs before adolescence begins(*16, 17*). Yet, while some studies have found that simple neuronal properties in the ACx (like response properties to pure tones) are nearly mature by adolescence, others report continued maturation well beyond this developmental stage(*14, 15*). For example, previous studies found that auditory learning and behavioral performance in auditory discrimination tasks involving amplitude modulation detection, as well as temporal interval discrimination tasks remain highly constrained during adolescence(*4, 5*). In those tasks, ACx neurons in adolescents exhibit high neuronal variability and lower tone sensitivity as compared to adults(*4*).

The perspective shift from viewing development as involving a set of discrete CPs to a broader view of continuous development with multiple, overlapping, CPs that affect each

other, calls for studies to test the extent of functional modulation in neuronal features after their CP closes. Thus, although the CP for pure tone representation in the ACx ends by ~P15, we hypothesized that learning of pure tone discrimination will remain malleable in adolescence, because other perceptual features and particularly other cognitive features are still developing. It remains unclear how these features are expressed when measured in the context of active behavior. We measured cortical activity in the ACx of adolescent mice engaged in an auditory discrimination task involving pure tones. Our findings show that learning, behavior, and sound representations to pure tones in the ACx are distinct in adolescence.

Results

Adult mice outperform adolescents on a difficult, but not an easy, auditory discrimination task of pure tones

To study learning and perceptual performance abilities we trained and tested adolescent and adult mice on an auditory pure-tone discrimination Go/NoGo paradigm. For this purpose, we utilized an automated behavioral platform called the 'Educage' (**Fig.1a**)(*18*). We trained adolescent (n = 15) and adult (n = 15) mice from post-natal day 20 (P20)-P37 and P60-P77, respectively (**Fig. 1b**). Following a tone association period (3-days; exposure to Go tones when mice enter the drinking port), mice learned to discriminate between two pure tones separated by 1 octave (7.07kHz *vs* 14.14kHz; **Fig. 1b-c**, light blue; herein referred to as the 'easy task'). After one week of training on the easy task (P23 to P30 in pre-adolescent mice and P63 to P70 in adult mice) mice were introduced to a second pure-tone pair, now separated by 0.25 octave (9.2kHz *vs* 10.9kHz) (**Fig. 1b-c**, dark blue; herein referred to as the 'hard task'). We completed the experiment after 1 week of learning on the easy and hard task simultaneously (i.e., at P37 for adolescent and P77 for adults). During the whole period of training, we also presented mice with low-probability, unrewarded 'catch' trials of pure-tones spanning the range of learned stimuli (**Fig. 1c**, grey). **Figure 1d** shows example learning curves (d') from one adolescent and one adult mouse over the 14-days course of tone discrimination. Adolescents and adults learned the procedure of the task similarly well, as measured by the number of trials it took mice to first reach threshold (d' value $\geq$ 1) (**Fig. 1e**).

We tested for differences in auditory discrimination by comparing the performance of mice along different epochs along training. First, by the end of the first week of training, all mice performed above the discrimination threshold (**Fig. 1f**). Although adolescent mice performed significantly less trials during the first week of training (**Fig. 1f**, vertical lines), there was no significant difference between the performance of adult and adolescent mice at the end of the first week (**Fig. 1f**, horizontal lines; d' calculated from the last 100 trials). Following one week of training on the easy task, we introduced the second pair of pure tones (**Fig. 1b**; 'Easy + Hard'). Immediately after introducing the hard pair, the performance of adolescent mice on the easy task dropped, while those of adults remained unaffected (**Fig. 1g**). During the second week of training adolescents regained their high d' values on the easy task, such that by the end of the experiment both groups had similarly high performance on the easy task (**Fig. 1h).**

We then compared how mice learned the hard task during the second week while training on both the easy and hard task simultaneously. While both groups now performed a similar number of trials (**Fig. 1i**, vertical lines), adult mice outperformed adolescent mice on the hard task (**Fig. 1i**, horizontal lines), suggesting the adolescents struggled with this (harder) level of discrimination. Indeed, on average, adolescent mice did not improve on the hard task

during the second week of training (**Fig. 1j**, adolescents). Adults, on the other hand, improved their performance on the hard task during the second week (**Fig. 1j**). Notably, neither group could learn the hard the task if it was not preceded by the easy task (**Fig. S1-1a-b**).

Although all mice trained for exactly 14 days, each mouse performed a unique number of trials, as these were initiated by the mice spontaneously. As noted above, pre-adolescent mice performed less trials/day as compared to adults but, notably, only during the first week of training (mean ± SEM: adolescents, 8317 ± 712 trials, adults 13229 ± 514 trials, t-stat = -5.6314, df = 28, p = 4.9566e-06, two-sample independent t-test). Still, this difference raises the question whether the different number of trials affected our conclusions from the first week of training. Thus, to evaluate the possible connection between the number of trials and performance in our data, we carried out several analyses. First, we found that the number of trials and d' were not correlated in either age-group during the first week of discrimination on the easy task (Pearson-r; adolescent: r = 0.1880, p = 0.5023; adult: r = -0.0730, p = 0.7959), nor on the second week of discrimination on both the easy and the hard task (Pearson-r; adolescent: r = 0. 2264, p = 0. 4171; adult: r = 0. 0194, p = 0. 9454). Second, we compared performance at three time points along the task with reference to times with shared number of trials: 1) evaluating d' after the minimal number of trials performed by all mice during the first week of training, and 2) evaluating d' at the mean number of trials of each group. We found no significant differences between adolescents and adults in all comparisons (**Fig. S1-1c-e**). Additionally, we found no significant differences between males and females, nor among experiments that had different numbers of co-housed mice in the Educage (**Table 1**). Taken together, despite the different absolute number of trials during the first week, we conclude that adolescents and adults learned the easy task equally quickly and effectively. The central difference between the age groups was in their ability to learn the hard task during the second week, when adults outperformed adolescents.

Adolescents have higher response bias and behavioral variability

We next asked what perceptual and/or cognitive aspect of behavior is different among the groups. We plotted psychometric curves based on both learned and catch trials from the last 2000 trials of the experiment (**Fig. 2a**). The false alarm rate but not the hit rate of adolescent mice was significantly higher as compared to adults (**Fig. 2b**). To calculate the decision boundary of mice and their perceptual sensitivity we normalized the psychometric curves of each mouse using a unity-based normalization and sigmoid fitting (**Fig. 2c**). We found no differences in the decision boundary or slopes of the curves, suggesting that perceptual sensitivities are not different between the groups (**Fig. 2c**). To test whether the differences arise from a cognitive effect (i.e., lick bias), we calculated the decision threshold as the maximal lick bias, also known as the criterion bias (C). C reflects the tendency to respond in a

liberal (i.e., negative C) or a conservative (i.e., positive C) manner to the sounds during the task. C was negative for both groups, yet significantly lower in adolescents, suggesting that their cognitive ability to withhold licking is inferior to that of adults (**Fig. 2d**).

Given that adolescents and adults show different dynamics in their performance along the task (**Fig. 1**), we tested whether the differences we found in lick bias are consistent or not across different times along the task. To normalize for different numbers of trials in each mouse, we divided their training episodes to the first and last tertiles during the first week and second week of training (**Fig.2e**). The maximal lick bias was significantly higher in adolescents in all but the very first training episode, when mice learned the procedure (**Fig. 2e-f**). These data highlight a general cognitive difficulty of adolescents to withhold licking during the task. The cognitive sensitivity of adolescents was further evident when their performance dropped right after the task was switched from 'easy only' to 'easy + hard' (**Fig. 1f**). The lick-bias of adolescent mice became significantly more biased after the introduction of the hard task (**Fig. 2g**). In contrast, the lick-bias of adult mice remained stable (**Fig. 2g**). These data further suggest that this cognitive trait (i.e., lick bias) has not yet matured in the young mice.

Prior studies have shown that a dominant feature of adolescent behavior is that it is more variable as compared to adults(*4*). To examine behavioral variability in our data, we calculated the coefficient of variation (CV) of the discriminability (d') for each mouse across training. While there was no significant difference in d' variability when training on the easy task during the first week of training (**Fig. 2h**), adolescent mice showed significantly higher variability during the second week of training while they trained on both the easy and hard tasks (**Fig. 2i,j**). Thus, adolescent learning and behavior are characterized by both lower response inhibition and higher variability, particularly during the second week when the task involved more challenging discriminations.

Adult mice outperform adolescent mice on a head-fixed discrimination task

To enable electrophysiological recordings during expert task performance, we trained adolescent (n = 5) and adult (n = 6) mice on a head-fixed learning paradigm, using a similar protocol as in the Educage (**Fig. 3a**). In the head-fixed protocol, water-access was limited to training sessions. Head-fixed mice were trained to lick after a 100ms tone and were rewarded (by water) or punished (by a 2 sec white noise) after a 600ms delay (**Fig. 3b**). Each session was concluded after mice became satiated and stopped licking. Water supply was limited to 0.0125 ml per day per gram of body weight, and mice that did not consume this amount were compensated after training (see Methods) (**Fig. 3c** shows an example session from one mouse). The number of trials per training session, was significantly lower in adolescents (mean ± SEM: adolescents: 410 ± 35, adults: 580 ± 37 t-statistic = -270.9855, p = 0.0012,

independent two-sample t-test). However, the number of sessions to reach the behavioral threshold (d' >= 1 in the easy task) was not significantly different between adolescents and adults (mean ± SEM: adolescents: 3.7 ± 0.8, adults: 3.8 ± 0.7; t-statistic = - 0.8531, p = 0.1971, independent two-sample t-test, **Fig. 3d**). While the number of trials performed within each session is likely related to physiological factors, such as smaller body weight and faster satiation, they did not impact learning capabilities. Similar to learning in the Educage, adolescent performance (but not that of adults) decreased after the introduction of the hard task (**Fig. 3e**). Another similarity between the head-fixed and EduCage versions of the task was that we found no significant differences between adolescents and adults in the performance of easy task (**Fig. 3f**), and that adults outperformed adolescents on the hard sound discrimination (**Fig. 3g**; compare to **Fig. 1h**).

To test whether ACx was necessary for expert discrimination in this task, we performed a causal experiment in adult mice. Adult mice (n=3) were injected bilaterally with AAV5-CAMKII-GtACR2-FRED_kv_2.1 into the ACx and optical fibers were implanted over the injection sites (**Fig. S3-1a, c**; **Fig. S3-2**). Mice were trained identically on the head-fixed Go/No-Go paradigm as described above. At the end of training, we attached a light source to the implanted fibers to allow optogenetic suppression during several sessions (**Fig. S3-1a**). In these sessions, light was applied in 50% of trials in a pseudo-random fashion, with light ON trials starting from -50ms prior to tone onset up to 50ms after tone offset (**Fig. S3-1b**). A control group of mice (n= 3) were injected with AAV9-CAMKII.H.dTomato and went through the exact same procedure (**Fig. S3-1a, c**). We compared the discriminability (d') for the easy and hard tasks under light-ON and light-OFF conditions. In GtACR2-injected mice (n = 13 sessions), but not in control mice (n=8 sessions), discriminability decreased significantly with optogenetic suppression for both the easy and hard tasks, although mice still performed better in the easy task under both conditions (**Fig. S3-1d**). Further, lick rates for both Go and No-Go stimuli were strongly affected in the GtACR2-injected mice, but not in controls (**Fig. S3-1e**). These results confirm findings by others in similar (though not identical) tasks (*19, 20*), suggesting that the ACx is necessary for execution of the behavior during the expert stage of this task.

To measure neural responses during behavioral performance, head-fixed expert mice underwent multiple recording-sessions targeting the ACx (adults, n = 14 recording sessions from 6 mice, age: P77-P82; adolescents, n = 13 recordings form 5 mice, age: P37-P42). During the recordings, the performance of all mice on the easy task was at least d'>1, and the d' on the hard task was smaller for both groups (often smaller than 1) (**Fig. S3-3a**). Performance was not significantly different across the multiple recording's sessions in each mouse (**Fig. S3-3b**). Behavioral performance during recordings was not significantly different to performance in the Educage (**Fig. S3-3c**). **Figure 3h** shows the evolution of

discriminability (d') during all recordings for adolescents and adults. Performance was heterogeneous across mice as well as within recording-sessions. However, the total number of trials performed was not significantly different (trials per recording: adolescent: 340.5 ± 45; adult: 431.1 ± 30.3; independent t-test, t-statistic = -203.7581, p = 0.1116).

We found a few differences between the behavior of adults and adolescents. The average adolescent discriminability was lower at the beginning of the session (initial 78 trials) but then rapidly leveled out (**Fig. 3i**). Adolescent mice had shorter lick latencies (**Fig. 3j, k**), and higher lick counts (**Fig. 3j, l; Supplementary Table 1**). While the lick latencies were independent of the discriminability (d'), we found a significant interaction-effect between lick count and the d' (**Supplementary Table 1**). Together, these behavioral differences suggest that the weaker response inhibition (here, expressed as lick latency) and higher reward anticipation (here, expressed as lick count) may contribute to the weaker performance of adolescents during the beginning of the recording.

Neuronal representations of stimulus- and choice-related activity are immature in adolescents

To compare between the activity of neurons in adolescent and adult mice, we recorded spiking activity from the ACx using the high-density Neuropixels-1 probes in expert mice engaged the task. We targeted the ACx by inserting the probe in a diagonal angle, traversing four auditory regions: Dorsal Auditory Cortex (AUDd), Primary Auditory Cortex (AUDp), ventral auditory cortex (AUDv), and Temporal Association Cortex (TEa) (**Fig. 4a** left**, Fig. S4-1a** shows one example recording). We recorded multiple times from each mouse and used DiI- or DiO-coatings for different penetrations to verify probe trajectories postmortem. We used the 3D-allen CCF-slice reconstruction (github.com/cortex-lab/allenCCF), for high resolution anatomical registration (**Fig.4a, b**; **Fig.S4-1b, c**).

We limited our single neuron analysis to well isolated single units from infragranular layer 5 and layer 6 (neurons from other layers and areas were excluded from the analysis), as two main projection layers of the cortex, which are key nodes for assessing cortical outputs(*21*). Together, we collected data from 1145 single neurons in 13 recordings of 5 adolescent mice and 1267 single neurons in 14 recordings of 6 adult mice (**Supplementary Table 2**). We further restricted our analysis to single neurons excited by sounds during the first 150ms after tone onset, to exclude the contribution of motor actions due to licking (**Fig. 4c**). Lick rate and FR-PSTHs were not correlated during the first 150ms (adolescents r = -0.1515 p = 0.9878; adults r = --0.0638 p = 0.9942). In total, we analyzed n=463 neurons in adolescent mice and n=599 in adults.

In Table 2, we present the number of neurons in our dataset, categorized by region. A detailed overview of the differences in firing properties per auditory region is provided in **Figure S4-2** and **Supplementary Table 3**. Consistent with previous work, we found that

firing properties such as minimal latency differed between auditory regions in both age-groups, with AUDp and TEa being most distinct (**Fig. S4-2, supplementary Table 3**) (*22*).

Notably, the effect size of the differences in baseline firing rates (FR) was larger in AUDd, AUDp, and AUDv. However, the evoked FR was smaller in all four areas. The coefficient of variance of the FR was larger in AUDd, AUDp, and AUDv. Additionally, the latency to peak was larger in AUDd and AUDp, while the full-width half maximum of the FR was also larger in these two areas. The minimal latency was larger in all four areas, and the number of responsive trials was smaller in all four areas. Finally, the lifetime sparseness (see Methods) was smaller in AUDp and AUDv between adolescent and adult neurons (**Supplementary Table 3**).

Next, to study how adolescents and adults encode task performance we divided neuronal responses by trial outcome (**Fig. 4d**). Specifically, we assessed neuronal discriminability between stimulus-related and choice-related activity by calculating the area under the curve (AUC) from a receiver operating curve (ROC) (**Fig. 4e**). Stimulus-related activity was calculated as the difference between hit and false alarm trials in the easy and the hard task separately. Choice-related activity was calculated as the average difference between false-alarm and correct reject trials (miss trials were excluded since we had insufficient trial numbers of this outcome). **Figure 4e** shows the average AUC values over time from an example neuron (same neurons shown in **Fig. 4D**), and **figure 4f** for all neurons. The onset-latency of discriminability was significantly slower, maximal discriminability significantly weaker, and the duration of discriminability significantly shorter in adolescent neurons compared to adult neurons (**Table 2**; plotted in **Fig. 4g**). We found no differences between auditory regions (**Fig. S4-3**). Thus, auditory processing of stimulus and choice related activity in the adolescent ACx are not fully mature.

Population decoding of the hard task in adults outperforms adolescents

While individual neurons exhibited weaker discriminability in adolescents than in adults, at a population level these effects could saturate out. We therefore tested the ability of recorded populations to decode trial outcome. We used a linear discriminant analysis (LDA) decoder to quantify hit versus correct reject trial outcomes, separately in easy trials and hard trials, based on population activity during the first 200 milliseconds. For the easy task there was no significant difference between decoding accuracy in adolescents and adults (**Fig. 5a**). However, decoding accuracy was significantly higher in adults compared to adolescents in hard trials (**Fig. 5a**). For both adults and adolescents decoding accuracy was significantly lower in hard trials compared to easy trials (**Fig. 5a**). We performed finer timescale decoding to quantify the onset latency of differences between the activity for hit vs. correct reject trials, defined as the time in which the decoding accuracy first crosses three times the standard

deviation away from the baseline (see Methods). We found that the latency was shorter in adults in both the easy and hard trials (**Fig. 5b**). In adolescent animals the latency was larger in hard trials (**Fig. 5b**) but not in adult animals (**Fig. 5b**). We then extended this analysis over a temporal window from -0.5s to10s relative to tone onset (**Fig. 5c**). In the 200ms window after the response period (2.0-2.2 s), there is no longer significant difference in decoding accuracy between adult and adolescent mice as well as between the two tasks (**Fig. S5-1**).

To further quantify the different decoding performance between two tasks, we plotted the fisher separation metric ($\frac{\sigma^2_{between}}{\sigma^w_{within}}$, see Methods) for each level of difficulty. The separation ratio of hard over easy tasks was significantly higher in adult mice than in adolescent mice (robust linear regression, see Methods). Separation could have changed due to alterations in the mean or the dispersion around the mean. Testing the dispersion, we found that the variance around the means was not equal across easy and hard trials but rather significantly increased for the hard trials (**Fig. 5d-f**). However, there was no significant difference in variance between adolescent and adult mice within the same task **(Fig. 5d-f**).

Effects of age and learning on cortical plasticity in mice engaged in the task

We next studied how learning contributes to cortical plasticity in the different age groups. To separate between age- and learning-related effects we recorded from the ACx of two new groups of mice (adolescents and adults) that are novice on the task (**Fig. 6a**, P38, recordings= 6; P78, recordings =6, n = 3 mice per group). We collected 130 tone-responsive (by excitation) neurons in novice adolescents and 186 tone-responsive (by excitation) neurons in novice adults (**Fig. 6b-c**; **Supplementary Table 2**). Notably, novice mice did not discriminate between sounds but were otherwise fully engaged in the task (**Fig. S61a-b**).

To reveal learning-related differences, we compared novice and expert mice of similar ages. We computed single-neuron AUCs for Go and No-Go trials (regardless of trial outcome) in both easy and hard stimulus pairs (**Fig. 6d-g**). The onset-latency for AUC discrimination was significantly different between adolescents and adults, but not between novice and expert mice, nor between the easy and the hard task. The maximal AUC discriminability was higher, and the duration longer in adults compared to adolescents, between experts and novice, and between the easy and hard tasks (**Table 3**). These results suggest that plasticity is reflected in the interaction of age and learning.

To compare between neuronal discriminability and behavior more explicitly, we analyzed the correlations between neuronal decoding and behavioral performance using linear regression. In the easy task, both age groups showed high correlation between neuronal discriminability and behavioral discriminability (**Fig. 6i, h**; light blue). In the hard task, only adult neurons had significant correlations between neuronal discriminability and behavioral

discriminability (**Fig. 6i, h**; dark blue). Taken together, our results show that cortical neurons in adults show greater improvements across learning.

Effects of age and learning on tuning properties in passively listening mice

Auditory discrimination learning has been shown to induce changes in the tuning properties of sounds in the ACx (*18, 21, 23-29*). To study whether learning-induced plasticity in ACx is distinct in adolescents and adults, we recorded from the same mice described above under passive listening condition, by simply extending the recording following the engaged session (**Fig. 7a, supplementary Table 5**; Adolescents recordings = 4; Adults recordings = 4). These data were compared to a group of novice mice, recorded under passive condition following their engaged session (**supplementary Table 5**; adolescent recordings =6; adult recordings =6).

We characterized the response profile of ACx neurons using a 'frequency-response area' protocol composed of twenty pure tones (4-40 kHz, spaced at 0.1661 octaves steps), each played for 100ms at five different attenuations (72-42 dB SPL). We limited our analysis to significant excitatory units only, determined as being auditory responsive in a window from tone onset to 50ms after tone offset at 62 dB SPL. Our dataset included four groups. The two adolescent groups were: 1) adolescent novice, and 2) adolescent experts, with 92 and 80 neurons, respectively. Two adult groups were: 3) adult novices, and 4) adult experts, with 123 and 84 neurons, respectively. Neurons in all groups responded to pure tone as expected from previous studies in adult mice, including classical V-shaped frequency response areas(*22, 30-33*). A representative example from a responsive neuron of the expert adolescent group and one from the expert adult group are shown in **figure 7b-c**. The peak of frequency tuning was heterogeneous across the frequency range with no clear trends of learning or age (**Fig. 7d**). To quantify these responses, we calculated tuning width (**Fig. 7e**), population sparseness (**Fig. 7f**), the distance between the best frequency of the neurons and the Go frequency of the easy task (**Fig. 7g**), and single neuron discriminability (**Fig. 7h**). As expected from previous work, learning significantly changed neuronal tuning properties in adults (**Fig. 7e-h**, 'Adults'). Surprisingly, however, learning had no significant effects on any of the single neuron parameters that we tested in the adolescent group (**Fig. 7e-h**, 'Adolescents'). Thus, despite the notion that adolescents' brains may be more plastic than adults, we found no clear evidence for learning-induced plasticity in basic tuning properties of the adolescent mice following our protocol (**Table 5, Fig. S6-1**). These results highlight that differences between adolescents and adults arise primarily from age and become more significant when the combined effects of age and learning are considered.

Discussion

The term "stormy adolescence" aptly captures what we know from psychology, neuroscience, and biology—that adolescence is a period of turbulent development, which shapes the individual's future behavior and health(*34, 35*). While numerous behavioral phenomena of adolescence have been studied, particularly in humans, the neural underpinnings of these remain largely unknown(*36*). In this study, we focused on (auditory) cortical neurons of the adolescent brain of mice while they were engaged in an auditory discrimination task. We found numerous differences in behavior, single neuron activity, and population encoding between adolescents and adults.

Adolescence behavior – perceptual and cognitive differences

We utilized the Educage platform to compare between adolescents and adults(*18*). The Educage provides an optimal environment for training young mice; its automated nature minimizes human handling, which increases efficiency and reduces to minimum any interference during the training process. Using the Educage, we found that procedural learning was intact in pre-adolescent mice (P20-P25), and behavioral differences were found only after the mice learned the task during the discrimination phase (P30-37). Compared to adults, adolescent mice scored lower on the hard versions of the task (**Fig. 1i-j**). Interestingly, our data suggests that the lower performance in adolescents was not due to a deficiency in perceptual sensitivity (**Fig. 2b**), but rather to a cognitive deficit– namely, response bias (**Fig. 2c**). This result is perhaps not surprising since higher response bias is a cognitive phenomenon that has been well documented in adolescence as a critical period of inhibitory control(*37*). Indeed, additional cognitive control mechanisms are still developing during this age(*38-40*).

Another manifestation of weaker cognitive control mechanisms is the noisy behavioral performance of adolescents (**Fig. 2h-j**). While this noise may reflect higher plasticity and potentially serve cognitive flexibility(*6, 41*), it poses a disadvantage for the precision and consistency required in our task. This noise may also arise from changes in pubertal hormones, which we did not manipulate(*42*). Notably, few studies have explicitly characterized auditory discrimination of adolescents in rodents; the majority of these have been carried out in gerbils using an amplitude modulation (AM) detection task (*4, 26, 43*). Despite the different task, many of our age-related findings are aligned with the findings in gerbils, including lower performance in adolescents, and greater variance in adolescent behavior(*4*). However, some findings differ. For example, the response bias which was different in our data, was similar between young and adult gerbils in an AM modulation detection task. This difference may arise from differences in task design, as well as the

severity of the punishment used in the task (here, we used a milder punishment). Together, our data support a view that cognitive factors, and to a lesser extent perception of pure tones *per se*, are the limiting factors in adolescent mice when performing a sound discrimination task.

Representation of stimulus and choice in ACx still undergoes maturation in adolescence

Motivated by the abovementioned behavioral differences, we tested how single neurons in ACx (which is necessary to perform our task, **Fig. S3-2**) represented sounds (by comparing Hits vs FA) and choices (by comparing FA to CR). Cortical representations of sounds in ACx could be the basis of perceptual constraints, while distinct processing of choices would reflect that more cognitive mechanisms are involved. We found differences in how cortical neurons represented both sounds and choices (**Figs. 4, 6, Tables 4-5**). In general, cortical representations of sounds and choices in mice engaged in the task were still immature as compared to adults, e.g., responses in adolescents were more sluggish and less informative (**Figs. 4-6**). These differences can be a result of age-related differences, and/or the result of a combined 'age x learning' effect.

We found purely age-related differences in single neuron activity between adolescents and adults (**Fig. 6d-g; Fig. 7**). But these age-related differences were quite small. This is perhaps not surprising because the CP for tonal organization in ACx is already completed by the time we tested the animals (i.e., on P38(*9, 13*)). We found more pronounced changes that are due to the combined effects of 'age x learning', which is expressed in mice that learned the task and are actively engaged in the behavior (**Fig. 4e, f; Fig. 6d-g**). We speculate that immature feedback (FB) to ACx may underlie these differences for several reasons. First, FB from higher cortical regions to more primary cortices has been proposed to be the neural substrate for hard perceptual discriminations(*44, 45*). Second, FB activity (also referred to as 'top down') is thought to be the key neural pathway involved in cognitive control mechanisms(*46*). FB is typically expressed in the late (>100ms) activity of single neurons, which was significantly different between adults and adolescents in our data (**Fig. 4d**). The exact source of FB that impacts perceptual or cognitive differences can arise from different brain regions that provide inputs to ACx(*47, 48*). Prefrontal cortical regions, like medial prefrontal cortex(*49, 50*), orbitofrontal cortex(*51*), or anterior cingulate(*52*) are the natural candidates; their causal contribution in adolescence should be tested in future experiments.

Cortical coding is performed by populations of neurons, which can efficiently encode stimuli on a trial-by-trial basis(*53-57*). Population coding, as measured here by decoding accuracy, largely recapitulated the results of the single neuron data. Specifically, cortical populations in adults encoded the different tones better and faster; particularly in the hard task

(**Fig. 5a-c**). Interestingly, by testing the quality (i.e., separation) of the decoding performance, we revealed a correlation between decoding in the easy and hard tasks in adult (**Fig. 5d**). This result suggests that the cortical network uses shared representation for decoding the easy and the hard tasks, possibly by the same neurons. This is consistent with our recent work showing that indeed the same neurons in ACx respond to the same stimulus differently, depending on if the mouse is engaged in discriminating an easy sound pair or a hard sound pair(*58*). The shallower slopes in adolescence suggest a less efficient decoding scheme that may arise from different populations of neurons encoding the stimuli in the easy and hard versions of the task.

Learning in the adolescent brain

Cortical representations of pure tones have a critical period (CP) between P12-P15(*13-15*). Indeed, we chose to study animals at P38-P40 on a pure tone discrimination task precisely to avoid the hypersensitivity associated with this CP. But this may be unavoidable, as recent work has shown that ACx also has a later CP for more complex sounds features(*14*, *15*). Those late CP's overlap with our training schedule and the underlying biological manifestation of this CP is expected to affect learning related plasticity in general. The underlying mechanism of the late CP to complex sounds has been associated with dynamic changes of inhibitory circuits(*59*, *60*). Thus, immature inhibitory circuits remain sensitive in adolescents, and could affect how pure tones are represented, despite the closure of the tonal CP. Notably, sound discrimination learning changes tonal representations in adults as well, which is well and beyond the CP's for all sort of sounds(*18*, *24*, *58*). We hypothesize, therefore, that age specific learning-related plasticity, rather than pure tone representation *per se*, shapes the differences in performance between adolescents and adults.

Taken together, we found that cortical responses of adolescents are different than those of adults after learning the exact same task to discriminate between pure tones and following the exact same protocol. Despite the natural closure of CPs for pure tones, learning to discriminate between tones is still different across age. How exactly the fine tuning of different CPs (e.g., the shaping of AM, or FM-sweep responses by inhibition) or the ongoing developmental maturation underlying cognitive controls (e.g., development of FB), contributes to distinct pure tone representations in a behaving animal remain open questions to explore. It is clear, however, that the ongoing developmental changes in the adolescent brain still impact its general performance in how simple sounds like pure tones are encoded. The adolescent-specific plasticity we found here taps directly onto how perceptual and cognitive features are represented in the ACx.

Acknowledgments:
We thank the Mizrahi lab for comments on the manuscript and Linda Wilbrecht, and Madeleine Klinger for discussions. We thank Ido Maor, Or Yudco, Omri Gilday, and Meirav Givon for technical assistance. We also thank Ofer Yizhar for sharing reagents and Maya Groysman for preparing the viruses. This work was supported by an NSF-BSF grant to A.M. and S.D. (#2021776), stipends from the Minerva Foundation and the Israeli Ministry of Aliya and Integration to B.P., and the Gatsby Charitable Foundation. Adi Mizrahi is the Eric Roland Chair in Brain Sciences. Figure 1a, 3a, S3a, 4a,7a were created with biorender.com.

Author Contributions:
B.P., and A.M. designed the experiments. B.P, A.D., and A.L., performed the experiments, B.P, F.C., S.D., analyzed the data. B.P., and A.M. wrote the paper with comments from F.C. and S.D.

Inclusion and Diversity:
We support inclusive, diverse, and equitable conduct of research

Declaration of Interests:
The authors declare no competing interests.

Supplemental information:

S1-1 *Behavioral criteria of auditory learning,* related to Figure 1.

S3-1 *Auditory Cortex is necessary for task execution in adult mice,* related to Figure 3.

S3-2 *Verification of GtACR2 expression,* related to Figure 3.

S3-3 *Adolescent and adult mice performed similarly throughout recordings as well as between the head-fixed configuration and the Educage,* related to Figure 3.

S4-1 *Probe reconstruction and activity profile across ACx regions,* related to Figure 4.

S4-2 *Adult and adolescent firing properties are distinct between auditory regions during task engagement,* related to Figure 4.

S4-3 *The neuronal discriminability of stimulus- and choice related activity is similar across auditory sub-regions,* related to Figure 4.

S5-1 *Decoding accuracy of the first 200ms after the response window,* related to Figure 5.

S6-1 *Behavioral performance of novice mice,* related to Figure 6.

Supplementary Table 1 *Adolescent and adult mice exhibit different lick behavior in the task,* related to Figure 3.

Supplementary Table 2 *Adolescent and adult firing properties are distinct between different sub-regions,* related to Figure 4

Supplementary Table 3 *Adolescent and adult mice have distinct firing properties in different sub-regions,* related to Figure 4

Supplementary Table 4 *Neuronal statistics during passive FRA protocol in expert and novice mice,* related to Figure 4.

Methods

Animals

A total of 47 (37 female and 10 male) C57BL/6 mice were used in this study. Adolescent mice were weaned at postnatal (P) day 20. Adult mice were trained starting from P60. All mice were housed on a 12-hour light / 12-hour dark cycle with food and water *ad lib*, unless used for behavioral training (see below). All experiments were approved by the Institutional Animal Care and Use Committee (IACUC) at the Hebrew University of Jerusalem, Israel (Permit Number: NS-21-16448-4, NS-21-16694-4, NS-22-16966-4).

Surgical procedures

The details for surgical procedures were identical to those used in previous studies from our laboratory (*18, 22, 47, 61-64*) . The relevant procedures are briefly described below.

RFID Implantation. 24h before the start of behavioral training in the automated home-cage, mice were implanted with a radio frequency identification (RFID) chip (Trovan, EX^{TM}). Animals were anesthetized with 2% Isoflurane with pure O2 as carrier. RFID chips were implanted under the scruff. After implantation, mice were injected with 0.04mg/g of 10 % Meloxicam solution to prevent infection and alleviate any possible pain from the implantation.

Head-bar Implantation & Craniotomy. 48h before the start behavioral training on the head-fixed recording set, mice were anesthetized with 2% Isoflurane, the body temperate maintained at 37 ° C and the eyes were covered with 5% Chloramphenicol ointment to prevent from drying. Before removal of the scalp, we applied 4% Lidocaine above the skin and skull area. Afterwards, we glued a custom-made titanium bar at the back of the mouse skull using dental cement (Meta-bond). To enable acute recordings in ACx, we performed a craniotomy on the left-hemisphere at 2.5 mm posterior and 4.0 lateral to the bregma. The craniotomy was protected by a pool of dental cement and covered with a silicon elastomer (WPI; Kwik-Cast catalog #KWIK CAST). After the craniotomy, mice were injected with 0.04mg/g of 10 % Meloxicam solution and 0.2 ml Saline. During the 48 hours of recovery, mice received two further doses of 0.04mg/g of 10 % Meloxicam solution. 24h before recordings, mice were again anesthetized to remove regrowth of the dura-mater during training. The area around the craniotomy was cleaned with Hydrogen-peroxide (3%), the silicon elastomer of the mice was replaced, and another dose of 10% Meloxicam was injected.

Virus Injection & Cannula Implantation. The surgical procedure was similar to the *head-bar implantation & craniotomy*. The differences in the procedure are outlined below. Bilateral craniotomies were performed at 2.5 mm posterior and 4.3 mm lateral to the bregma. We injected 200nl AAV5-CAMKII-GtACR2-FRED_kv_2.1, or 200nl AAV9-CAMKII-dTomato. Both viruses were produced at the ELSC virus-core facility. We injected the virus at a depth of 1.1 mm at 0°. Afterwards, we inserted a 0.2 mm diameter optical fiber with an attached cannula (CFML1202; Thorlabs) at a depth of 0.9 mm at 0°, bilaterally. We chronically fixed the fiber position on the skull using dental cement (Meta bond).

Auditory Stimuli

Sound stimuli were delivered from a calibrated free-field speaker (ES1 SN:4568) using a multifunction processor (ED1; Tucker-Davis Technologies). The speakers were calibrated with a free-field microphone (Type 4939, Bruel and Kjaer). The stimuli were comprised of pure tones, sampled at 500 kHz, between 7.07 to 14 kHz for behavioral training and 4-40 kHz for passive listening. All stimuli were played at sound pressure levels of 72 dB SPL for behavioral training, and 72-, 62-, 52-, and 42-dB SPLs for passive listening. All tones were played in randomized order.

Behavior

Automated home-cage training (the 'Educage'). For a detailed description of the EduCage behavioral platform, see (*18*). After RFID- implantation, groups of 5 mice were placed in their home-cage that was connected to a behavioral chamber called the Educage (Fig. 1a). Mice were provided with food *ad libitum*. Water access was restricted to the Educage chamber. Mice could access the Educage freely to retrieve water mixed with 5% sucrose. The behavioral training was controlled by a custom LabView 2019 (National Instruments) program running on BNC-2110 (National Instruments) and FPGA (MyRIO – National Instruments) to register licks, RFIDs numbers, and deliver stimuli and reinforcements. Every time a mouse entered the water port its RFID was automatically recognized, a trial initiated, and an auditory stimulus played from a speaker vertically positioned above the behavioral chamber. We trained mice gradually for three weeks on a Go/No-Go paradigm of pure tones, spaced around a category boundary of 10 kHz. This paradigm enabled us to efficiently compare between adolescent and adult behavior, since learning was restricted from post-weaning (P20) to adolescence (P37) (correspondingly adults were trained from P60-P77). Mice were trained in four separate training phases (Fig. 1B). For the first 24h (P20-P21 in the adolescent group of mice and P60-P61 in adult mice) mice were habituated to the behavioral chamber and could approach the port freely to retrieve water after licking the waterspout (0.0015 ml per trial). During the following 48h (P21-P23 in the adolescent group of mice and

P61-P63 in adult mice) mice underwent a tone-association phase. All tones played were 300ms long (sampled at 500 kHz). Tone association was restricted to the lowest Go tone (7.07 kHz at 100% probability). Mice received a water-reward in response to licking during the first 3 seconds after tone-offset. This was followed by the first tone-discrimination stage, which contained a No-Go tone (14.14 kHz at 45% probability) at 1 octave (octave) away from the Go tone. We analyzed four response outcomes—Hits, Misses, Correct Rejections, False Alarms— in the 2.5 seconds response window after the tone-offset. 'Hits' were counted after 5 successful licks to the Go-tone and followed by a water-reward. 'Misses' were counted when licks to the Go-tone trials did not pass the lick threshold. Correspondingly, 'Correct Reject' (CR) trials, were all No-Go trials below the lick threshold. CR trials were not reinforced. 'False Alarms' (FA) were counted when 5 or more licks were registered after the No-Go. FA trials were followed by a white-noise punishment (5-20 kHz at 72 dB SPLs, 2 seconds) and an inter trial delay of 5 seconds. In addition, mice were exposed to 5 catch trials (tones whose trial outcome that were neither rewarded nor punished at 8.49 kHz, 9.567 kHz, 10 kHz, 10.44 kHz, and 11.89 kHz; played at 2% per tone). Mice trained on the 1 octave tone discrimination for 1 week (P23-P30 in adolescent mice and P63-P70 in adult mice). Next, we added a second pair of tone - a Go/No-Go tone pair spaced 0.25 octaves apart (9.17 kHz and 10.95 kHz) for another week of training. The experiment was terminated at age P37 for adolescent and P77 for adult mice.

Head-fixed training. We used a head-fixed paradigm that enabled us to efficiently train adolescent and adult mice on the same task and record from engaged mice after learning. We trained mice on the same Go/No-Go stimulus set of the Educage described above with few differences which are outlined below.

The head-fixed behavioral training was controlled by a custom MATLAB 2023B (Mathworks) program running on BNC-2110 (National Instruments) to register licks and deliver stimuli and reinforcements. Mice were water-restricted for 24h prior to training, and their weight monitored daily. While training on the set, mice received water supplemented with 5% sucrose, depending on their weight (0.125 ml per g of body weight). Additional water, in the form of Hydrogel (ClearH2O) was given after daily training if mice did not consume the required amount during training, or their body weight dropped below 85% of the pre-restriction weight. Mice were gradually habituated to the set by head-fixation and received free water after licking, during the first training day (P23 in adolescent mice and P63in adult mice). Licking was measured with an optical lick-meter (Sanworks). During the second training day mice were associated with a tone. All tones of the task were 100ms long (sampled at 500 kHz). Mice received a water reward in response to licking in the first 2 seconds after tone offset. Reward-reinforcement was delayed to 0.5 seconds after the tone

offset. To break the regularity of the trial sequences, we applied a dynamic inter-trial interval of 6-8 seconds. New trials were initiated if mice did not lick the spout at least 2 seconds prior to the upcoming trial. Mice were familiarized with the tone for at least two training days (P24-26 in adolescent mice and P64-66 in adult mice). Then, and when the lick rate was above 80%, mice proceeded to the first tone discrimination stage. We gradually increased the probability of No-Go trials, depending on the lick rate of the mouse. We added the 0.25 octave Go/ No-Go tone pair, after a maximal of seven training days on the 1 octave tone pair (P26-33 in adolescent mice and P66-73 in adult mice), or if the behavioral performance exceeded a threshold of d' = 1, as calculated using the signal detection metric. Mice were trained until P37 in the adolescent group and P77 in the adult group.

Optogenetic Manipulation

Adult mice (P60) were injected with AAV5-CAMKII-GtACR2-FRED_kv_2.1 (n = 3) and implanted with cannulas prior to training as described above. Mice underwent optogenetic stimulation after training on the head-fixed task by attaching a ferrule patch cable (M79L01; Thorlabs) to the implanted cannula using a mating sleeve (ADAF1; Thorlabs). The ferrule cable end (SMA connector) was connected to an LED driver setup (LEDD1B; Thorlabs) that enabled us to send precise outputs at 476 nm (blue light; 5mW) bilaterally. To test the effect ACx inhibition on task performance, we timed the LED output to 50ms before tone onset until 50ms after tone-offset. The LED consisted of pulses given at 10 Hz for 200ms

Behavioral sessions of optogenetic manipulation were identical to the Go/No-Go paradigm of previous training sessions. We inhibited ACx in 50% of the trials in randomized order. Optogenetic manipulations were repeated throughout multiple sessions of expert performance. As a control, we repeated the same experiment in mice injected with AAV9-CAMKII-dTomato (n = 3). After completion of the experiment, animals were deeply anesthetized with Ketamine-and medetomidine (0.008 g/kg, and 0.65 mg/kg, respectively) and then perfused with 4% Paraformaldehyde. After the perfusion, the brain was extracted and preserved. We then sectioned the ACx using a cryostat (Leica) into 0.05 mm thick coronal slices. Afterwards brain slices were washed one time under 1% Phosphate-buffered saline (PBS), and a second time with 1% PBS plus 0.4% Triton. Finally, slides were mounted and stained with DAPI (4%) and imaged using a wide-field fluorescent microscope (Olympus Life Science, Olympus IX83), to reconstruct the probe position offline.

Extracellular Recordings

Recording set-up. Before the onset of the recording session, we removed the silicon elastomer and placed an external reference electrode (Ag/AgCl wire) on the skull of the right hemisphere. All recordings were performed using Neuropixels 1.0 (Npx; IMEC, phase 3A), a

base-station connected to a chassis (IMEC; NI PXIe -1071, National Instruments). Probes were mounted to a custom-made steel rod and connected to the ground. Before penetration, probes were covered with a fluorescent dye (Dil (Invitrogen catalog #V22885- red, or Dio (Invitrogen catalog #V22886 – yellow), to reconstruct penetration sites after the recording. Then, Npx probes were inserted into the left ACx at 30° to a depth of 3.85 mm. The skull surface was submerged in saline and the probe allowed to settle for 10 min. We sampled recordings at 20 kHz, with action potential band filtered to contain 0.3- to 10kHz frequencies. Action potential band gain was set to 500. Out of the 960 available sites on the 1cm shank of the Npx probe (*65*), we acquired the 384 lowest recording shanks in a staggered configuration. We used common-average referencing to process the voltage-traces.

Recording Schedule. We performed recordings of both naïve and expert adolescent and adult mice. Naïve recordings were performed after tone-association (see *head-fixed training;* adolescent n=3; adult n = 3). Expert recordings were performed after learning (adolescent n= 5; adult n = 6). Both naïve and expert recording include the easy (1 octave) and hard (0.25 octave) tone pair. Both recordings were performed after P37 for adolescent mice and P77 for adult mice. Tone probabilities and protocol parameters were identical to the *head-fixed training*. Each mouse was recorded multiple times (naïve recordings adolescents n = 6; naïve recording adults n =6; expert recordings in adolescents n = 13; expert recordings in adults n = 14). In some mice, after the recording in the engaged configuration, we recorded neural activity under passive listening conditions to a pure tone protocol (naïve recordings adolescents n = 5; naïve recording adults n = 5; expert recordings in adolescents n = 4; expert recordings in adults n = 4). The pure tone protocol was comprised of 20 different frequencies, logarithmically spaced between 4 and 40 kHz, presented at 5 sound pressure levels (see *Auditory stimuli*). Each frequency and attenuation combination were presented 16 times. The tone interval was set to 1 second. After completion of the recording schedule, animals were deeply anesthetized with Ketamine and medetomidine (0.008 g/kg, and 0.65 mg/kg, respectively) and perfused with 4% Paraformaldehyde. After the perfusion, we performed histological analysis and sectioned coronal brain slices as described above (see *Optogenetic Manipulation*) in order to reconstruct the exact probe position**.**

Preprocessing & Spike-sorting. All recordings were sorted using Kilosort 2.5/3 open-source software ((*66*) ; https://github.com/MouseLand/Kilosort). After automatic sorting, we performed manual curation of the acquired units using 'Phy-2' open-source GUI. (UCL; https://github.com/cortex-lab/phy). During manual curation we distinguished between single units (SUs) and noise (pre-labeled multi-units in Kilosort2.5/3 were automatically labelled as noise). The following parameters were set to determine SUs: physiologically plausible

waveform shape (1–2 ms, biphasic/triphasic), high spike-amplitude (> 50 µV, SNR > 3), physiologically plausible refractory period (ISI > 4ms), sufficient inter-spike-interval (ISI peak 5–10 ms), sufficient firing-rate across the recording (>0.1 spikes/sec), and principal-component cluster density (high density and low overlap). In addition, SUs were compared to neighboring units, based on waveform, firing rate, drift-pattern and cross-correlograms to determine merging of two SUs into a single cluster (Pearson Correlation Coefficient >0.8). Units that passed the above-mentioned criteria were considered single units (SUs).

Data Analysis

The analysis was performed with MATLAB R2023b (MathWorks) and Python3.13 (PyCharm 2024.1.3). In all figures, unless mentioned otherwise, we represent mean and median of the data, together with standard deviation, quartile, or standard error of the mean (MAD/sqrt(n); n = number of data points).

Behavioral analysis. We categorized behavioral responses of the task into hit, miss, false alarm, and correct reject responses. To compare behavioral performance, we calculated the d' value based on the signal detection metric (d' = the inverse normal distribution of the z-scored hit rate) – the z-scored (false alarm rate)). D' values of 0 were rounded to 0.01 and d' =1 was rounded to 0.99, to avoid values approaching infinity. We applied a gaussian-smoothing filter (bin-size = 100 trials) to evaluate the d' learning trajectory (Fig 1d., supplementary Fig.1.3 a, c). Concrete d' values of naïve and expert performance are reported unfiltered (Fig. 1 f, g; supplementary Fig.1.1 b; supplementary Fig.1.2 a; Fig. 2 d, e). Next, we calculated psychometric curves based on the lick-rate to learned and catch trials (Fig. 1h.). Psychometric curves were normalized and fitted to a sigmoidal function, defined as followed:

$$S(t) = a\frac{1}{1+e^{\frac{-(t-b)}{c}}} \qquad \text{(Equation 1)}$$

Where *a* denotes the lick-rate, *b* = the time of the infliction point, and *c* = the steepness of the curve. Based on the normalized psychometric curve, we extracted two infliction points (random lick rate at 0.5 and category boundary at 10 kHz; Fig. 1i). To compare the heterogeneity of adolescent and adult behavior, we calculated the lick bias (the inverse normal distribution of the z-scored (hit rate) + z-scored (false alarm rate; Fig. 1j) and analyzed the coefficient of variation (CV) of behavior across the learning (supplementary Fig. 1.3). We applied similar behavioral measurements to the Educage training and head-fixed training, as well as recordings and optogenetic manipulation during task performance. During expert-

performance in the head-fixed task, we analyzed the running d' as the average performance of the last 25 trials (Fig. 2, f-g). In addition, we also calculated the average lick trace during the reinforcement delay. Here, we also extracted the lick latency per trial per mouse, defined as the lick latency from tone-onset (Fig. 2i).

Neuronal analysis. Probe trajectories and location of SUs were reconstructed using Allen CCF tools (https://github.com/cortex-lab/allenCCF ; (*67*)). For further analysis we only considered SUs that were recorded from infragranular layers 5 and layer 6. SUs from the dorsal-auditory cortex (AUDd), primary auditory cortex (AUDp), ventral auditory cortex (AUDv) and temporal association cortex (TEa) were pooled together as auditory cortex (ACx), and in some analyses presented separately(*62*). Neurons were considered excitatory auditory responsive if the average spontaneous firing rate (FR) of the baseline activity preceding the tone (200ms to 50ms before stimulus onset) was significantly lower than the average tone-related activity (from stimulus onset until 50ms after stimulus offset) across all trials (*22*). The difference was tested with a right-sided Wilcoxon sign rank test ($p < 0.05$). Suppressed auditory responsive units and non-auditory responsive units were excluded from the analysis. Peri-stimulus time histograms (PSTHs) were smoothed with a gaussian smoothing filter of 5ms. To test the difference between adolescent and adult auditory firing properties in expert mice, we calculated the difference in average spontaneous FR (-200ms preceding the tone onset until tone-onset, average evoked FR (tone onset until 50ms after tone offset) and fraction of responsive trials. We also compared the coefficient of variance of the evoked FR (mean FR divided by standard deviation of the FR across trials). Temporal differences in firing properties were compared by calculating the latency to peak (latency of the highest FR), minimal latency (first spike after tone-onset), full-width-half-maximum (FWHM; time from peak FR to baseline FR), and the lifetime sparseness, which was calculated as follows:

$$S = \left(1 - \left(\frac{(\frac{\sum r_i}{n})^2}{\frac{\sum r_i^2}{n}}\right)\right) / (1 - \frac{1}{n}) \qquad \text{(Equation 2)}$$

r_i = corresponds to the FR of each learned frequency and n equals the number of learned tones. Values of S near 0 correspond to a dense FR and values near 1 to a sparse code (*68*).

Single neuron analysis during task performance. We investigated the FR of excitatory auditory responses per trial from 200ms preceding the stimulus upto 600ms after the tone onset. To test how well single neurons discriminate between trial outcomes, as well as task-

difficulty, we calculated task-related activity per trial using receiver operating characteristics (ROC) and calculated the area under the curve (AUC) across a running window of 25ms in bins 50ms (Fig. 4, Fig. 6). Stimulus-related activity was defined as the hit compared to the false alarm trials, separately for the 1 octave and 0.25 octave tone pair. Stimulus-related activity of miss compared to correct trials were not analyzed due to the lack of miss trials in expert performance. In addition, we also tested the average (mean of 1 octave and 0.25 octave tone pair) choice discrimination, defined as the difference between false alarm and correct reject trials (Fig. 4). We sampled 20 trials per trial outcome and repeated the ROC encoding 100 times. Afterwards, we adjusted the average AUC values of all iterations of each neuron to its baseline AUC before the tone onset ((AUC – baseline AUC) + 0.5). AUC values close to 0.5 indicate a low neuronal discriminability, and values approaching 1 indicate high neuronal discriminability (*69*). To test significant discrimination, we repeated the ROC encoding with shuffled trial identities (20 randomly shuffled trials per trial outcomes across 100 iterations). Significant discriminability of a neuron was defined as the AUC time bins that exceed the mean ±3 std of the shuffled distribution (*61*). Adolescent and adult neuronal discriminability were compared using the onset-latency of discrimination of a neuron (first timepoint > mean ±3 std of the shuffled distribution; Fig. 4h, Fig. 6c), the maximal AUC of the running window (Fig. 4j, Fig. 6e) and the duration of discriminability (time duration > mean ±3 std of the shuffled distribution; Fig. 4i, Fig. 6d). To compare naïve and expert performance we repeated the AUC encoding and compared the general discrimination of 1 octave and 0.25 octave Go and No-Go discrimination of all trial outcomes (Fig. 6). To evaluate the correlation of behavioral performance and neuronal discriminability, we compared d' per recording to the average of the maximal AUC all of neurons per recording. The AUC and d' values were compared via pairwise Pearson correlation (Fig. 6f).

Auditory cortex population analysis during task performance. We investigated the FR of excitatory auditory responses per trial from 200ms preceding the stimulus up to 600ms after the tone onset. To test how well single neurons discriminate between trial outcomes, as well as task-difficulty, we encoded task-related activity per trial using ROC and calculated the AUC across a running window of 25ms in bins 50ms (Fig. 4, Fig. 6). We then compared stimulus-related activity, defined as hit compared to false alarm trials in the 1 octave and 0.25 octave tone pair. Stimulus-related activity of miss compared to correct trials were not analyzed due to the lack of miss trials in expert performance. In addition, we also tested the average (mean of 1 octave and 0.25 octave tone pair) choice discrimination, defined as the difference between false alarm and correct reject trials (Fig, 4). We sampled 20 trials per trial outcome and repeated the ROC-encoding 10 times. Afterwards, we adjusted the average AUC values of all iterations of each neuron to its baseline AUC before the tone onset (AUC –

baseline AUC) + 0.5). To test significant discrimination, we repeated the ROC encoding with shuffled trial identities (20 randomly shuffled trials per trial outcomes across 10 iterations). Significant discriminability of a neuron was defined as the AUC- time bins that exceed the mean ±3 std of the shuffled distribution (*61*). Adolescent and adult neuronal discriminability were compared using the onset-latency of discrimination of a neuron, the maximal AUC of the running window, and the duration of discriminability. To compare naïve and expert performance we repeated the AUC encoding and compared the general discrimination of 1 octave and 0.25 octave Go and No-Go discrimination of all trial outcomes (Fig. 6). Finally, we compared d' per recording to the average of the maximal AUC all of neurons per recording. The AUC and d' values were compared via pairwise Pearson correlation (Fig. 6f).

Auditory cortex population analysis during task performance. We analyzed the population activity in the ACx of adolescent and adult mice on a trial-by-trial basis. Population activity was segregated by hit and correct-reject trials for both easy and hard tasks in each age group. We excluded recordings that contained fewer than 20 auditory-responsive neurons, fewer than 20 hit or correct-reject trials in either task. This resulted in a total of 8 adolescent sessions and 10 adult sessions. To decode the stimulus from neural activity, we applied linear-discriminant analysis (LDA) to the first 200ms following stimulus onset. Decoding accuracy was calculated on held-out trials (10 trials per stimulus) (Fig. 5a). To examine changes in decoding accuracy over time, we used a 50ms bin width and fitted separate LDA models at each time point, covering a period from -0.5s to 10s after stimulus onset (Fig. 5c). Next, we computed the separation per session, defined as the ratio of the between-class variance to the within-class variance. Given the means μ_1, μ_2 and variances Σ_1, Σ_2 of the two classes, the separation is given by:

$$S = \frac{\sigma^2_{between}}{\sigma^2_{within}} = \max_w \frac{\left(w(\mu_1 - \mu_2)\right)^2}{w^T(\Sigma_1 + \Sigma_2)w}. \qquad \text{(Equation 3)}$$

We used robust linear regression without intercept (Huber loss) to fit the relationship between separations in easy and hard tasks (Fig. 5d). To quantify when the decoding accuracy is significantly different from the baseline, we used a 50ms bin width with a sample frequency of 100 Hz. Baseline decoding accuracy was calculated as the mean and variance of decoding accuracy during a 500ms window before stimulus onset, up to 50ms before onset. Decoding latency was defined as the time from stimulus onset to the first time point where decoding accuracy exceeded three standard deviations from the baseline mean (Fig. 5b). One adolescent session, in which behavioral d' is less than 1, has decoding accuracy that does not exceed three standard deviations from the baseline mean within the first 200 ms. Therefore, this session was excluded from the latency analysis. Finally, we assessed the single-trial variance across both age groups and tasks. Data were standardized per neuron before computing

variance per stimulus (Fig. 5e). To visualize the results, we projected the population representations to the space spanned by the two LDA decoding dimensions for the easy and hard tasks. We averaged the mean and covariance matrix across sessions for each stimulus and age group, representing the distributions with corresponding ellipses (Fig. 5f).

Single neuron analysis during passive listening. We extracted the frequency-response areas (FRAs; Fig. 7b) based on the pure-tone responses (from tone onset up to 50ms after tone-offset) of auditory responsive neurons. The bandwidth of excited units was computed for significant responses at 62 dB SPL and subtracted by the number of expected false-positive responses. We then calculated the population sparseness as the fraction of significant excited responses in adolescent and adult naïve and expert mice (Fig. 7f). To test the neuronal discriminability to pure tone responses, we calculated the pairwise d' based on the FR per trial in all frequencies at 62 dB SPL (*22, 63*). For two given frequencies p and q, d' values were calculated in the following way:

$$\frac{d(\mu_{p,}\mu_q)}{\mu(\sqrt{\sum_n^{i=1}(\widehat{p_i}-\widehat{q_i})^2})} \qquad \text{(Equation 4)}$$

Where d represents the distance between the mean FR (μ) of frequency p and q, as vectors with n entries representing the mean signal (averaged over individual trials) in n-dimensional space for frequency p/q. The average distance (d) is then divided by the mean of the inner Euclidian distance ($\sqrt{\sum_n^{i=1}(\widehat{p_i}-\widehat{q_i})}$) between each single trial (Fig. 7g).

Statistical Analysis. Statistical comparisons were performed in custom-written codes in MATLAB 2023b (MathWorks) and Python 3.12. We assessed if the data was normally distributed using a Kolmogorov-Smirnov test. Normally distributed data was tested using a paired (within group comparison) or independent (between group comparison) t-test and presented with mean ± SEM. Non-normally distributed data was tested using a Wilcoxon sign rank (within group comparison), or rank-sum (between group comparison) test. Multiple-samples were tested with ANOVA (parametric data) and Kruskal-Wallis tests (non-parametric data). All tests corrected after multiple comparisons (Bonferroni-correction for two-samples and Tukey-Kramer for multiple samples). In addition we applied linear-mixed-effect models (LME) to account for hierarchical data structures and variability within groups of co-housed mice (Table 1), repeated measurements of mice and recordings (supplementary Table 1 , Table 3, Table 4), as random effects. Fixed effects, and pairwise interaction-effects were adjusted with post-hoc tests and multiple comparisons. For all statistical tests significant differences were defined as p-values below 0.05.

897

Figure Legends

Figure 1: *Adolescent mice exhibit lower performance during self-initiated auditory learning in the 'Educage'.* **A**. Schematic model of the 'Educage' (left), the trial structure and trial types (FA, false alarm; CR, correct reject). **B.** Experimental timeline. Total training time was 21 days (±2). **C.** The sounds used for training. Light blue- easy task; dark blue- hard task; Grey- catch-trials. **D.** Learning curve examples. Adolescent mouse (left, P20-to-P37); adult mouse (right, P60-to-P77). Vertical dashed lines indicate the easy-hard transition. Horizontal line is d'=1. **E.** Number of trials to reach threshold (d'>=1; adolescents, n =15; adults, n=15; z=-0.1659; p=0.8682, two-sample Wilcoxon rank sum test). **F.** Discriminability (d') of the easy task in adolescent mice at P30 (grey; n=15, d'=2.0001±0.1791; n trials=8317±712) and adult mice at P70 (black; n=15, d'=2.1986 ± 0.2441; n trials=13229 ± 514, top: marked by the arrowhead). Dashed lines: mean trials per group (t-stat=-5.6314, df=28 ,p=4.9566e-06, two-sample independent t-test, vertical line), and mean d' per age group (z=-0.2074; p=0.8357, two-sample Wilcoxon rank sum test, horizontal line) **G.** Change in discriminability (Δd') of the easy task before and after the introduction of the hard task (Top: arrowheads; left: adolescent, signed rank=14, p=0.0067; right: adult, signed rank=14, p=0.1514, one-sample Wilcoxon signed rank test; Δd' between adult and adolescent mice: z=-2.0739; p=0.0381, two-sample Wilcoxon rank sum test) **H.** Same as 'G' for the first 100 and last 100 trials of the experiment in the easy task (adolescent signed rank=120, p=6.1035e-05; adult signed rank=120, p=6.1035e-05, one-sample Wilcoxon signed rank test; Δd' between adult and adolescent mice: z=-1.0370; p=0.2998, two-sample Wilcoxon rank sum test). **I.** Same as 'F' for the hard task (adolescent-grey; n=15, d'=1.1895±0.1783; n trials=4163 ± 297; adult-black; n=15, d'=1.8342 ± 0.1743; n trials=4102±475) (mean trials per group: t-stat=0.1306, df=28, p=0.8970, two-sample independent t-test, vertical line; mean d' per group: z=-2.2398; p=0.0251, two-sample Wilcoxon rank sum test, horizontal line). **J.** Same as 'G' for the hard task. (adolescent signed rank=73, p=0.4887; adult signed rank=114, p=8.5449e-04, one-sample Wilcoxon signed rank test; Δd' between adult and adolescent mice: z=-1.9495; p=0.0512, two-sample Wilcoxon rank sum test).

Figure 2*: Adolescent mice exhibit lower response inhibition and higher variability in performance over the course of learning.* **A.** Schematic timeline of tone discrimination). **B.** Average psychometric curve of the lick rate across all stimuli (catch and learned; No-Go stimuli: p = 0. 0085, Go stimuli: p = 0. 0963, Wilcoxon rank sum test, after Bonferroni correction). **C.** Same as 'B', but normalized and fitted to a sigmoid function0(lick rate at 10kHz, p = 0.1163; frequency at 50% lick rate, p = 0.5896, Wilcoxon rank sum-test, after Bonferroni correction). **D.** Maximal lick bias (i.e., criterion bias) per mouse during the last 2000 trials (c-bias: p = 0.0136, Wilcoxon rank sum test). **E.** Average psychometric curve, fitted to a sigmoid function across all stimuli (catch and learned) at different periods of the experiment — Left: first tertile-easy task (per mouse; adolescent n = 15, adult n = 15); Middle-left: last tertile – easy task; Middle-right: first tertile-hard task; Right: last tertile-hard task. (Dashed vertical =category boundary). **F.** Same as E. as the maximal C-bias. From left to right:(z = -0.5104, p = 0.6098, two-sample Wilcoxon rank sum test), (z = -2.6546, p = 0.0079, two-sample Wilcoxon rank sum test), (z = -4.0739, p = 4.6228e-05, two-sample Wilcoxon rank sum test), (z = -3.2768, p = 0.0011, two-sample Wilcoxon rank sum test). **G.** Change in lick bias (Δ c-bias) between the last 100 trials before and after the introduction of the hard task. (left, adolescent signed rank = 17, p = 0.0125; right, adult signed rank = 83, p = 0.2078, one-sample Wilcoxon signed rank test; Δ c-bias between adolescents and adults, z = -2.9035; p = 0.0037, two-sample Wilcoxon rank sum test). **H.** Coefficient of variation (CV) of the d' of the easy task before the introduction of the hard task. (z = -0.1659, p = 0.8682, two-sample Wilcoxon rank sum test) **I.** Same as 'H' after the introduction of the hard task (z = 2.1569, p = 0.0310, two-sample Wilcoxon rank sum test). **J.** Same as 'H' but for d' of the hard task (z = 2.5302, p = 0.0114, two-sample Wilcoxon rank sum test).

Figure 3: *Adolescent mice exhibit lower performance in the head-fixed discrimination task.* **A.** Experimental timeline of training followed by recordings. **B.** Trial structure during the recording. Solid lines indicate the tone period. Dashed lines show the reward or punishment delay (0.6 sec), and the response window (2 sec). **C.** Example session. Licks (grey ticks) and trial outcomes (hit = green, false alarm = yellow, miss = red and correct reject = blue) across all trials in one recording session. **D.** Discriminability during training sessions for the easy task (light blue) and hard task (dark blue). **E.** Change in d' after the introduction of the hard task (last 100 trials of the last session of the easy task compared to last 100 trials of the first hard session; rank-sum = 14; p = 0.0381, two-sample Wilcoxon rank sum test). **F.** Expert d' of the last 100 trials during the last training session of the easy task (rank-sum = 21; p = 0.1255, two-sample Wilcoxon rank sum test). **G.** Same as 'F', but for the hard task (rank-sum = 17; p = 0.0173, two-sample Wilcoxon rank sum test). **H.** Behavioral performance (average d' of the easy and the hard task) per mouse during recording sessions for adolescents (n =13, left) and adults (n= 14, right) (trials per recording: adolescent: 340.5385 ± 45.0650; adult: 431.1429 ± 30.3367; independent t-test, t-statistic = -203.7581, p = 0.1116). **I.** Same as 'H' but only for the first 148 trials. The color bar shows the p-values between the groups. **J.** Average cumulative licks per trial in adolescents (dashed-line) and adults (solid-line) from -200ms before tone -onset until the reward or punishment delay, 500ms after tone-offset. **K.** Lick latency per trial for adolescent (left) and adult (right) groups during electrophysiological recordings (LME statistics are shown in **supplemental Table 1**). **J.** Same as 'K' for the Lick count.

Figure 4: ACx *neurons in adolescents exhibit lower discriminability in stimulus- and choice-related activity* **A.** Recordings in ACx when the mouse is engaged in the task, using Neuropixels-1 probes. Left: Recordings were performed in AUDd, AUDp, AUDv, and TEa. Right: Fluorescent micrograph of a coronal brain slice showing the probe tracks of three recordings (red = DiI, yellow = DiO). **B.** Top: 3D-Reconstruction of recording sites in adolescents (n = 13; light green) and adults (n = 14; dark green). Bottom: distribution of the spike-depth of all excitatory tone-responsive L5/6 neurons in adolescents (n = 455; light green) and adults (n = 607; dark green). **C.** Normalized PSTH and lick-rate (LR) from -200ms to +600ms after tone-onset in adolescents (light green) and adults (dark green). **D.** Spiking activity from one example neuron sorted by trial outcome (hit, miss, false alarm, correct reject). Top: PSTH per trial outcome. Bottom: Heat map of the FR sorted pertrial outcome. **E.** Discriminability values (AUC) over time (from -200ms to 600ms after tone onset) for one example neuron (same neuron as in 'D'). AUC values are shown for stimulus related activity (left: easy task, middle: hard task) and choice-related activity (right). Shuffled distribution in all curves is shown in grey. **F.** Same as 'E' for all neurons. The curves are average (+- SEM) neuronal discriminability of adult neurons (solid line) and adolescent neurons (dashed line), for easy (adolescent neurons = 190, mice = 4, recordings = 7; adult n = 358, mice = 4, recordings = 8; left) and hard stimulus-related activity (adolescent n = 429; adult n = 562 , mice = 5, recordings = 9; middle), and choice-related activity (adolescent n = 429; adult n = 562 , mice = 5, recordings = 9; right). **G.** 3D plots of the onset- latency of discriminability (ms), duration of discriminability (ms), and maximal discriminability (AUC) of all neurons that showed significant discriminability. Left: easy task (adolescent neurons = 178, mice = 4, recordings = 6; adult n = 346, mice = 4, recordings = 8; left); Center: hard task (adolescent neurons = 368, mice = 5, recordings = 10; adult n = 544, mice = 6, recordings = 12; middle); Right: choice-related activity (adolescent neurons = 368, mice = 5, recordings = 10; adult n = 544, mice = 6, recordings = 12; right).

Figure 5: *Decoding in adult neuronal populations outperforms decoding in adolescents.* **A.** Decoding accuracy for the first 200ms across all recordings in both adults (dark green) and adolescents (light green) for the easy task (adolescents compared to adults, p=0.5000, Student's t-test) and the hard task (adolescents compared to adults, p=0.0300, Student's t-test).

Decoding is better in the easy task for both age groups (adults: p=0.0030; adolescents: p=0.01, paired t-test). **B.** Decoding latency for all recordings in the easy task (p=0.0200, Student's t-test) and the hard task (p=0.0030, Student's t-test), as well as compared between age groups (easy task, p=0.05400, pared t-test; hard task: p=0.0100). **C.** Decoding accuracy over a time window from -0.5s to 10s. **D.** LDA separation for easy and hard tasks. Lines represent robust linear regression fits without intercept (Huber loss; robust linear regression, p=0.0001) **E.** Single trial variance for easy and hard tasks in adolescent and adult recordings (adults: p=0.0040; adolescents: p=0.0300, paired t-test; easy task: p=0.4500; hard task: p=0.4100, Student's t-test). **F.** Visualization of population representations for the stimuli in easy and hard tasks. Dotted lines indicate decoding dimensions, and ellipses represent the covariance of the representations.

Figure 6: *Cortical activity during behavior reflects both age- and learning-induced effects.* **A.** Training and recording schedule for novice mice, compared to expert mice. **B.** 3D-Reconstruction of recording sites in novice adolescent (n = 6; light green) and novice adult (n = 6; dark green) mice. Bottom: spike-depth of excitatory tone-responsive L5/6 adolescent (n = 107; light green) and adult (n = 177; dark green) neurons. **C.** Normalized FR and lick-rate (LR) PSTH from -200ms to 600ms after tone-onset in adolescents (light green) and adults (dark green). Average +-sem. **D.** Single neuron data from novice adolescent mice. Left: Heat map of the FR per trial from one example neuron sorted by trial outcomes. Center: the AUC of the neuron from the left for the easy and hard stimulus pairs (light and dark blue, respectively). Right: Average (+-SEM) AUC of all neurons in the novice group (n = 140 neurons). **E-G.** Same as 'D' for novice adult (n = 186 neurons), expert adolescents (n = 455 neurons; Easy vs hard), and expert adults (n = 604 neurons; Easy vs hard.). **H.** Linear regression analysis between the average AUC per recording and the behavioral d' during the recording (the correlation and p values are indicated for each plot). **I.** Same as 'I' for adult mice.

Figure 7: *Unlike adults, neuronal tuning properties of adolescents do not change after learning* ***A.*** Schematic showing that for the passive listening protocol, we continued our recording following the session of the engaged task (i.e. in satiated mice) by removing the waterspout. **B.** Example raster plot of a neuron from an adolescent mouse (top) and an adult mouse (bottom). **C.** FRA's of the neurons shown in 'B'. **D.** Distribution of best frequencies in our dataset. Values are normalized firing rates calculated at 62 dB SPL. Matrices are sorted by BF for clarity. Dotted line marks the decision boundary. **E**. Tuning bandwidth at 62 dB SPL of neurons in adolescents and adults. Side by side comparisons of novice versus experts. (adolescents p = 0.0882, adults p = 0.0001, Kruskal Willis Test after Tukey-Kramer correction for multiple comparisons). **F**. Same as E. for the Population sparseness (adolescents p = 0.9549, adults p = 0.0013, Kruskal Willis Test after Tukey-Kramer correction for multiple comparisons). **G** Same as E. for the distance (in octaves) between the best-frequency of each neuron to the easy Go-stimulus (adolescents p = 0.0816, adults p = 0.6391, Kruskal Willis Test after Tukey-Kramer correction for multiple comparisons). **H** Same as E. for the average neuronal d' of frequencies in the learned frequency spectrum (adolescents p = 0.1627, adults p = 0.0026, Kruskal Willis Test after Tukey-Kramer correction for multiple comparisons).

Main Tables

Table 1: *Behavioral differences between adolescent and adult mice are age-, but not sex-related.* Fixed effects of age and sex, and the random effects of co-housing in the 'Educage' on the discriminability (mean d' of the last 100 trials of the easy and hard task to avoid pseudo replication) of all mice (Number of observations = 30, Fixed effects coefficients = 3, Random effects coefficients = 7, Covariance parameters = 2). Coefficient estimates, STE, T-statistic, degrees of freedom, p-values (adjusted for multiple comparisons with the Bonferroni

method) and the lower and upper Confidence Interval (95%). The model includes random effects coefficients of the Cage ID in each group of co-housed mice (7 cages in total; see *methods*, equation 7).

Table 2: *Neuronal discrimination is later, shorter, and less precise in adolescent neurons.* Linear mixed effect models of the neuronal discriminability in adolescence and adulthood per stimulus-related activity in the easy task (Number of observations = 524, Fixed effects coefficients = 2, Random effects coefficients = 10, Covariance parameters = 3), stimulus related activity in the hard task (Number of observations = 943, Fixed effects coefficients = 2, Random effects coefficients = 14), and choice-related activity (Number of observations = 520, Fixed effects coefficients = 2, Random effects coefficients = 10, Covariance parameters = 3). The table shows the fixed effects of the coefficient estimates, STE, T-statistic, degrees of freedom, p-values (corrected for multiple comparisons with Bonferroni-correction) and the upper and lower CI of the effect of age on the onset latency of discrimination, duration of discrimination and maximal neuronal discrimination (AUC). Each model also included random effect coefficients of each mouse, and recording per mouse. P-values for were adjusted with post-hoc tests using Bonferroni-correction (see *methods*, equation 9).

Table 3: *The effect of age, learning and task difficulty on the latency, duration, and ability to discriminate tones in ACx neurons.* Linear mixed effect models of the effect of age, learning and task difficulty on onset-latency of discrimination, duration of discrimination and maximal discriminability (Number of observations = 2590, Fixed effects coefficients = 8, Random effects coefficients = 20, Covariance parameters = 3). The table shows the fixed effects of the coefficient estimates, STE, T-statistic, degrees of freedom, p-values (corrected for multiple comparisons with Bonferroni-correction) and the upper and lower CI. The model also includes random effects coefficients of each mouse (adolescent novice = 3, adult novice = 3, adolescent expert = 5, adult expert = 6) and recording per mouse (n = 3). P-values for were adjusted with post-hoc tests using Bonferroni-correction (see *methods*, equation 10).

Supplementary Figure Legends

Supplementary Figure 1-1: *Behavioral criteria of auditory learning.* **A.** Learning curves per mouse throughout the experiment (n=5 adolescents, n=4 adults). **B.** Discriminability of novice (first 1000 trials) compared to "expert" (last 1000 trials) mice in the adolescent and adult groups (Novice vs Expert — Adolescents, p = 0.0625; Adults, p = 0.0625, Wilcoxon sign ranked test after Bonferroni correction; Adolescents vs Adults — Novice, p = 0.4444, Expert, p = 0.5476, Wilcoxon rank sum test after Bonferroni correction. **C.** Discriminability (d') of the easy task at the minimal number of trials (5087 trials) shared between all mice (z = -1.0370; p = 0.2998, two-sample Wilcoxon rank sum test). ***D.*** Discriminability (d') of the easy task at the mean number of trials of adolescent mice (8317 trials) shared between all mice (n = 15 per group) (z = 0.9125; p = 0.3615, two-sample Wilcoxon rank sum test). E. Same as A. but for the mean number of trials (13229 trials) of adult mice (adolescent n =4; adult n = 15) (z = 0.9125; p = 0.5304, two-sample Wilcoxon rank sum test).

Supplementary Figure 3-1: *Auditory Cortex is necessary for task execution in adult mice* **A.** Experimental design for testing the role of ACx during tone discrimination in expert mice (Adults only). **B.** Protocol for transient optogenetic suppression (light pulse duration was -50ms to +150ms from tone onset). **C.** Injection sites and optical fiber implantation for the experimental (GtACR2; top) and control groups (CAMKII; bottom). **D.** Behavioral performance (d') per session under light OFF conditions in easy (light blue) and hard (dark blue) task, as compared to light ON conditions (red) in experimental (GtACR2, n = 13 ; top ; easy task: p = 0.0010, hard task: p = 0.0007, two-sample Wilcoxon rank sum test after Bonferroni correction; light on p = 0.0010; light off: p = 0.0398, one-sample Wilcoxon sign

ranked test after Bonferroni correction) and control mice (CAMKII n = 8; bottom, easy task: p = 0.9999, hard task: p = 0.7422, two-sample Wilcoxon rank sum test after Bonferroni correction;; light on p = 0.0312; light off: p = 0.0234, one-sample Wilcoxon sign ranked test after Bonferroni correction). **E.** Lick rate for Go and No-Go stimuli under light OFF conditions (grey) as compared to light ON conditions (red) in experimental (GtACR2, n = 13; top; Go stimuli: p = 0.0001; No-Go stimuli: p = 0.0107; one-sample Wilcoxon sign ranked test after Bonferroni correction) and control mice (CAMKII, n = 8; bottom; Go stimuli: p = 0.4263; No-Go go stimuli: p = 0.2953; one-sample Wilcoxon sign ranked test after Bonferroni correction).

Supplementary Figure 3-2: *Verification of GtACR2 expression*. Photomicrograph (left), and reconstruction (right) of the GtACR2 infected area (red) per mouse. Reconstruction followed the coordinates of the Allen-CFF template-atlas with ACx highlighted in white and GtACR2 in red.

Supplementary Figure 3-3: *Adolescent and adult mice performed similarly throughout recordings as well as between the head-fixed configuration and the Educage.* **A.** Behavioral performance (d') in the easy task (light blue) and hard task (dark blue) for adolescent (recording = 13; left) and adult (recording = 14; right) recordings at the behavioral criterion of d' >1 (adolescent mice: signed rank: 91, p = 2.4414e-04; adult mice: signed rank: 105, p = 1.2207e-04, Wilcoxon sign ranked test). Behavioral threshold of d' = 1 highlighted in the dashed line. **B.** Behavioral performance (average d' of the easy and the hard task) for every mouse per recording for adolescent mice (n = 5; left; 1st rec.: p = 0.8125; 2nd rec.: p = 0.9999; 3rd rec.: p = 0.9999, Wilcoxon sign ranked test, after Bonferroni correction). and adult mice (n =6; right; 1st rec.: p = 0. 8438; 2nd rec.: p = 0.9999; 3rd rec.: p = 0.9999, Wilcoxon sign ranked test, after Bonferroni correction). Behavioral threshold of d' = 1 highlighted in the dashed line. **C.** Comparison of behavioral performance in the head-fixed configuration and the Educage for adult mice (left; easy task: p = 0.9960; hard task: p = 0.2159, Kruskal Wallis test after Bonferroni correction), and adolescent mice (right; easy task: p = 0.9973; hard task: p = 0.1505, Kruskal Wallis test after Bonferroni correction) in the easy (light blue) and the hard (dark blue) task.

Supplementary Figure 4-1: *Probe reconstruction and activity profile across ACx regions.* **A.** 3D-Reconstruction of recording sites in adolescent (n = 5; left) and adult (n = 6; right) mice. **B.** Example PSTH per depth (50 μm bins) across AUDd, AUDp, AUDv and TEa (3850 maximal depth μm). **C.** Spike-depth of excitatory tone-responsive L5/6 neurons in AUDd, AUDp, AUDv and TEa of adolescent (top) and adult (bottom) recordings. **D.** Population PSTH from – 200ms to 600ms after tone onset in AUDd (blue), AUDp (purple), AUDv (magenta) and TEa (green) for adolescent neurons (dashed line) and adult neurons (solid line).

Supplementary Figure 4-2: *Adult and adolescent firing properties are distinct between auditory regions during task engagement* **A.** Adolescent average baseline FR of excited single neurons in AUDd (blue), AUDp (purple), AUDv (magenta) and TEa (green) from tone-onset to 50ms after tone offset across all stimuli. Average baseline FR (Hz, statistical comparisons are presented in supplementary Table 2) **B.** Same as A. for the evoked FR (Hz) **C.** Same as A. for coefficient of variance of FR **D.** Same as A. for the latency to peak of maximal FR (ms).**E.** Same as A. for the full-width-half maximum of peak FR (ms) **F.** Same as A. for the minimal latency of peak FR (ms). **G.** Same as A. for proportion of responsive trials. **H.** Same as A. for the lifetime sparseness. **I-P.** Same as A-H. for adult neurons.

Supplementary Figure 4-3: *The neuronal discriminability of stimulus- and choice related activity is similar across auditory sub-regions* Onset- latency of discriminability (ms), duration of discriminability (ms), and maximal discriminability (AUC) of neurons that showed significant discriminability (exceeded 3 STD of the shuffled distribution), in the easy

(adolescent neurons = 178, mice = 4, recordings = 6; adult n = 346, mice = 4, recordings = 8; left), and hard stimulus related discriminability (adolescent neurons = 368, mice = 5, recordings = 10; adult n = 544, mice = 6, recordings = 12; middle), , and choice-related activity (adolescent neurons = 368, mice = 5, recordings = 10; adult n = 544, mice = 6, recordings = 12; right) across the AUDd, AUDp, AUDv and TEa neurons.

Supplementary Figure 5-1: *Decoding accuracy of the first 200ms after the response window.* LDA decoding accuracy the easy and the hard task of adolescent and adult mice 200ms after the response window.

Supplementary Figure 6-1: *Behavioral performance of novice mice* **A.** Behavioral performance (d') in the easy task (light blue) and hard task (dark blue) for adolescent (n = 6; left) and adult (n = 6; right) mice at the behavioral criterion of d' >1 (adolescent mice: signed rank: 19, p = 0.0938; adult mice: signed rank: 15, p = 0.4375, Wilcoxon sign ranked test). Behavioral threshold of d' = 1 highlighted in the dashed line. **B.** Behavioral performance (average d' of the easy and the hard task) for every mouse per recording for adult mice (n = 3; left; signed rank: 0, p = 0.2500 Wilcoxon sign ranked test). adolescent mice (n = 3; right; signed rank: 0, p = 0.2500, Wilcoxon sign ranked test). Behavioral threshold of d' = 1 highlighted in the dashed line.

Supplementary Tables

Supplementary Table 1. *Adolescent and adult mice exhibit different lick behavior in the task.* Linear mixed-effects models of the fixed effects of lick count (until reward or punishment delay), lick latency, cumulative discriminability (d') (including the interaction effects of lick count and lick latency, lick count and d', lick latency and d', and lick latency, lick count and d') during the minimal number of trials shared between all mice (148 trials; Number of observations = 1098, Fixed effects coefficients = 8, Random effects coefficients = 14, Covariance parameters = 3). Coefficient estimates, STE, T-statistic, degrees of freedom, p-values (adjusted for post-hoc multiple comparisons with Bonferroni-method), lower and higher CI are listed in the table. The model includes random effects coefficients per mouse (11 mice in total) and 3 recordings per mouse (see *methods, equation 8*).

Supplementary Table 2: *Neuronal statistics in expert and novice recordings during task engagement.* Acquired single units, acquired tone-excited units (fraction of tone-excited units) in the AUDd, AUDp, AUDv, and TEa of adolescent and adult mice in experts (top) and novice (bottom).

Supplementary Table 3: *Adolescent and adult firing properties are distinct between different sub-regions.* P-values of Kruskal Willis Test after Tukey-Kramer correction for multiple comparisons of the average baseline FR (Hz), evoked FR (Hz), coefficient of variance of FR, latency to peak of maximal FR (ms), full-width-half maximum of peak FR (ms), minimal latency of first spike (ms), fraction of responsive trials, lifetime sparseness of all adolescent and adult neurons from tone-onset to 50ms after tone offset across all stimuli AUDd – AUDp, AUDd – AUDv, AUDd – TEa, AUDp – AUDv, AUDp – Tea, and AUDv – Tea (significant p-values are highlighted in bold).

Supplementary Table 4: *Adolescent and adult mice have distinct firing properties in different sub-regions.* Mean and standard error, mean effect size (robust Cohen's D), lower and upper Confidence Interval (CI) and p-value (Wilcoxon rank-sum test, adjusted for multiple comparisons with Bonferroni method) of the average baseline FR (Hz), evoked FR (Hz), coefficient of variance of FR, latency to peak of maximal FR (ms), full-width-half

maximum of peak FR (ms), minimal latency of first spike (ms), fraction of responsive trials, lifetime sparseness of all adolescent and adult neurons from tone-onset to 50ms after tone offset across all stimuli in AUDd, AUDp, and AUDv, and TEa (significant p-values are highlighted in bold).

Supplementary Table 5: *Neuronal statistics during passive FRA protocol in expert and novice mice*. Acquired single units, acquired tone-modulated units, and fraction of modulated units to all acquired units in the AUDd, AUDp, AUDv, and TEa of adolescent and adult mice during passive-listening recordings.

Declaration of generative AI and AI-assisted technologies in the writing process:
During the preparation of this work the author(s) used ChatGPT in order to edit the text for spelling and grammar. After using this tool/service, the author(s) reviewed and edited the content as needed and take(s) full responsibility for the content of the publication.

Data availability
The data that support the finding of this study are available through Zenodo (https://zenodo.org/uploads/13933351). Additional data is available from authors upon reasonable request.

Code availability
The code is available through GitHub (https://github.com/benne1295/Age-and-Learning-Shapes-Sound-Representations-in-Auditory-Cortex-During-Adolescence).

References

1. D. Hoskins, Consequences of Parenting on Adolescent Outcomes. *Societies* **4**, 506-531 (2014).
2. J. D. Hawkins, R. F. Catalano, J. Y. Miller, Risk and protective factors for alcohol and other drug problems in adolescence and early adulthood: implications for substance abuse prevention. *Psychol Bull* **112**, 64-105 (1992).
3. D. Fuhrmann, L. J. Knoll, S. J. Blakemore, Adolescence as a Sensitive Period of Brain Development. *Trends Cogn Sci* **19**, 558-566 (2015).
4. M. L. Caras, D. H. Sanes, Neural Variability Limits Adolescent Skill Learning. *J Neurosci* **39**, 2889-2902 (2019).
5. J. J. Huyck, B. A. Wright, Late maturation of auditory perceptual learning. *Dev Sci* **14**, 614-621 (2011).
6. C. Johnson, L. Wilbrecht, Juvenile mice show greater flexibility in multiple choice reversal learning than adults. *Dev Cogn Neurosci* **1**, 540-551 (2011).
7. D. Romer, Adolescent risk taking, impulsivity, and brain development: implications for prevention. *Dev Psychobiol* **52**, 263-276 (2010).
8. L. Wilbrecht, J. Y. Davidow, Goal-directed learning in adolescence: neurocognitive development and contextual influences. *Nat Rev Neurosci* **25**, 176-194 (2024).
9. T. K. Hensch, Critical period plasticity in local cortical circuits. *Nat Rev Neurosci* **6**, 877-888 (2005).
10. T. K. Hensch, Critical period regulation. *Annu Rev Neurosci* **27**, 549-579 (2004).
11. R. K. Reh, B. G. Dias, C. A. Nelson, 3rd, D. Kaufer, J. F. Werker, B. Kolb, J. D. Levine, T. K. Hensch, Critical period regulation across multiple timescales. *Proc Natl Acad Sci U S A* **117**, 23242-23251 (2020).
12. A. Kral, Auditory critical periods: a review from system's perspective. *Neuroscience* **247**, 117-133 (2013).
13. T. R. Barkat, D. B. Polley, T. K. Hensch, A critical period for auditory thalamocortical connectivity. *Nat Neurosci* **14**, 1189-1194 (2011).
14. S. Bhumika, M. Nakamura, P. Valerio, M. Solyga, H. Linden, T. R. Barkat, A Late Critical Period for Frequency Modulated Sweeps in the Mouse Auditory System. *Cereb Cortex* **30**, 2586-2599 (2020).
15. M. Nakamura, P. Valerio, S. Bhumika, T. R. Barkat, Sequential Organization of Critical Periods in the Mouse Auditory System. *Cell Rep* **32**, 108070 (2020).
16. Y. J. Sun, G. K. Wu, B. H. Liu, P. Li, M. Zhou, Z. Xiao, H. W. Tao, L. I. Zhang, Fine-tuning of pre-balanced excitation and inhibition during auditory cortical development. *Nature* **465**, 927-931 (2010).
17. L. I. Zhang, S. Bao, M. M. Merzenich, Persistent and specific influences of early acoustic environments on primary auditory cortex. *Nat Neurosci* **4**, 1123-1130 (2001).
18. I. Maor, R. Shwartz-Ziv, L. Feigin, Y. Elyada, H. Sompolinsky, A. Mizrahi, Neural Correlates of Learning Pure Tones or Natural Sounds in the Auditory Cortex. *Front Neural Circuits* **13**, 82 (2019).
19. S. K. Talwar, G. L. Gerstein, Reorganization in awake rat auditory cortex by local microstimulation and its effect on frequency-discrimination behavior. *Journal of neurophysiology* **86**, 1555-1572 (2001).
20. S. K. Talwar, P. G. Musial, G. L. Gerstein, Role of mammalian auditory cortex in the perception of elementary sound properties. *Journal of Neurophysiology* **85**, 2350-2358 (2001).
21. P. O. Kanold, I. Nelken, D. B. Polley, Local versus global scales of organization in auditory cortex. *Trends Neurosci* **37**, 502-510 (2014).

1299 22. L. Feigin, G. Tasaka, I. Maor, A. Mizrahi, Sparse Coding in Temporal Association
1300 Cortex Improves Complex Sound Discriminability. *J Neurosci* **41**, 7048-7064 (2021).
1301 23. S. Bao, E. F. Chang, C. L. Teng, M. A. Heiser, M. M. Merzenich, Emergent categorical
1302 representation of natural, complex sounds resulting from the early post-natal sound
1303 environment. *Neuroscience* **248**, 30-42 (2013).
1304 24. S. Bao, E. F. Chang, J. Woods, M. M. Merzenich, Temporal plasticity in the primary
1305 auditory cortex induced by operant perceptual learning. *Nat Neurosci* **7**, 974-981
1306 (2004).
1307 25. Y. K. Han, H. Kover, M. N. Insanally, J. H. Semerdjian, S. Bao, Early experience impairs
1308 perceptual discrimination. *Nat Neurosci* **10**, 1191-1197 (2007).
1309 26. K. L. Anbuhl, J. D. Yao, R. A. Hotz, T. M. Mowery, D. H. Sanes, Auditory processing
1310 remains sensitive to environmental experience during adolescence in a rodent
1311 model. *Nat Commun* **13**, 2872 (2022).
1312 27. S. Jaramillo, A. M. Zador, The auditory cortex mediates the perceptual effects of
1313 acoustic temporal expectation. *Nat Neurosci* **14**, 246-251 (2011).
1314 28. H. K. Kato, S. N. Gillet, J. S. Isaacson, Flexible Sensory Representations in Auditory
1315 Cortex Driven by Behavioral Relevance. *Neuron* **88**, 1027-1039 (2015).
1316 29. C. O'Sullivan, A. P. Weible, M. Wehr, Auditory Cortex Contributes to Discrimination
1317 of Pure Tones. *eNeuro* **6**, (2019).
1318 30. G. Rothschild, I. Nelken, A. Mizrahi, Functional organization and population dynamics
1319 in the mouse primary auditory cortex. *Nat Neurosci* **13**, 353-360 (2010).
1320 31. L. Cohen, A. Mizrahi, Plasticity during motherhood: changes in excitatory and
1321 inhibitory layer 2/3 neurons in auditory cortex. *J Neurosci* **35**, 1806-1815 (2015).
1322 32. L. Cohen, G. Rothschild, A. Mizrahi, Multisensory integration of natural odors and
1323 sounds in the auditory cortex. *Neuron* **72**, 357-369 (2011).
1324 33. I. Maor, A. Shalev, A. Mizrahi, Distinct Spatiotemporal Response Properties of
1325 Excitatory Versus Inhibitory Neurons in the Mouse Auditory Cortex. *Cereb Cortex* **26**,
1326 4242-4252 (2016).
1327 34. S. M. Sawyer, R. A. Afifi, L. H. Bearinger, S. J. Blakemore, B. Dick, A. C. Ezeh, G. C.
1328 Patton, Adolescent Health 1 Adolescence: a foundation for future health. *Lancet*
1329 **379**, 1630-1640 (2012).
1330 35. L. P. Spear, Neurobehavioral changes in adolescence. *Current Directions in*
1331 *Psychological Science* **9**, 111-114 (2000).
1332 36. R. E. Dahl, N. B. Allen, L. Wilbrecht, A. B. Suleiman, Importance of investing in
1333 adolescence from a developmental science perspective. *Nature* **554**, 441-450 (2018).
1334 37. L. M. Reynolds, L. Yetnikoff, M. Pokinko, M. Wodzinski, J. G. Epelbaum, L. C. Lambert,
1335 M. P. Cossette, A. Arvanitogiannis, C. Flores, Early Adolescence is a Critical Period for
1336 the Maturation of Inhibitory Behavior. *Cereb Cortex* **29**, 3676-3686 (2019).
1337 38. H. C. Meyer, D. J. Bucci, Age differences in appetitive Pavlovian conditioning and
1338 extinction in rats. *Physiol Behav* **167**, 354-362 (2016).
1339 39. L. Magis-Weinberg, R. Custers, I. Dumontheil, Rewards Enhance Proactive and
1340 Reactive Control in Adolescence and Adulthood. *Soc Cogn Affect Neurosci* **14**, 1219-
1341 1232 (2019).
1342 40. J. R. Cohen, R. F. Asarnow, F. W. Sabb, R. M. Bilder, S. Y. Bookheimer, B. J. Knowlton,
1343 R. A. Poldrack, A unique adolescent response to reward prediction errors. *Nat*
1344 *Neurosci* **13**, 669-671 (2010).
1345 41. E. A. Crone, R. E. Dahl, Understanding adolescence as a period of social-affective
1346 engagement and goal flexibility. *Nat Rev Neurosci* **13**, 636-650 (2012).
1347 42. T. Kunkhyen, E. Perez, M. Bass, A. Coyne, M. J. Baum, J. A. Cherry, Gonadal
1348 hormones, but not sex, affect the acquisition and maintenance of a Go/No-Go odor
1349 discrimination task in mice. *Horm Behav* **100**, 12-19 (2018).

1350 43. B. N. Buran, E. C. Sarro, F. A. Manno, R. Kang, M. L. Caras, D. H. Sanes, A sensitive
1351 period for the impact of hearing loss on auditory perception. *J Neurosci* **34**, 2276-
1352 2284 (2014).
1353 44. M. Ahissar, S. Hochstein, The reverse hierarchy theory of visual perceptual learning.
1354 *Trends Cogn Sci* **8**, 457-464 (2004).
1355 45. M. Ahissar, S. Hochstein, Task difficulty and the specificity of perceptual learning.
1356 *Nature* **387**, 401-406 (1997).
1357 46. E. Zagha, Shaping the cortical landscape: functions and mechanisms of top-down
1358 cortical feedback pathways. *Frontiers in Systems Neuroscience* **14**, 33 (2020).
1359 47. G. I. Tasaka, L. Feigin, I. Maor, M. Groysman, L. A. DeNardo, J. K. Schiavo, R. C.
1360 Froemke, L. Luo, A. Mizrahi, The Temporal Association Cortex Plays a Key Role in
1361 Auditory-Driven Maternal Plasticity. *Neuron* **107**, 566-579 e567 (2020).
1362 48. G. I. Tasaka, C. Maggi, E. Taha, A. Mizrahi, The local and long-range input landscape
1363 of inhibitory neurons in mouse auditory cortex. *J Comp Neurol* **531**, 502-514 (2023).
1364 49. K. Delevich, M. Klinger, N. J. Okada, L. Wilbrecht, Coming of age in the frontal cortex:
1365 The role of puberty in cortical maturation. *Semin Cell Dev Biol* **118**, 64-72 (2021).
1366 50. X. Konstantoudaki, K. Chalkiadaki, E. Vasileiou, K. Kalemaki, D. Karagogeos, K.
1367 Sidiropoulou, Prefrontal cortical-specific differences in behavior and synaptic
1368 plasticity between adolescent and adult mice. *J Neurophysiol* **119**, 822-833 (2018).
1369 51. C. M. Johnson, F. A. Loucks, H. Peckler, A. W. Thomas, P. H. Janak, L. Wilbrecht, Long-
1370 range orbitofrontal and amygdala axons show divergent patterns of maturation in
1371 the frontal cortex across adolescence. *Dev Cogn Neurosci* **18**, 113-120 (2016).
1372 52. E. M. Nabel, Y. Garkun, H. Koike, M. Sadahiro, A. Liang, K. J. Norman, G. Taccheri, M.
1373 P. Demars, S. Im, K. Caro, S. Lopez, J. Bateh, P. R. Hof, R. L. Clem, H. Morishita,
1374 Adolescent frontal top-down neurons receive heightened local drive to establish
1375 adult attentional behavior in mice. *Nat Commun* **11**, 3983 (2020).
1376 53. S. Druckmann, D. B. Chklovskii, Neuronal circuits underlying persistent
1377 representations despite time varying activity. *Curr Biol* **22**, 2095-2103 (2012).
1378 54. B. Kang, S. Druckmann, Approaches to inferring multi-regional interactions from
1379 simultaneous population recordings: Inferring multi-regional interactions from
1380 simultaneous population recordings. *Curr Opin Neurobiol* **65**, 108-119 (2020).
1381 55. N. Li, K. Daie, K. Svoboda, S. Druckmann, Robust neuronal dynamics in premotor
1382 cortex during motor planning. *Nature* **532**, 459-464 (2016).
1383 56. Z. Wei, H. Inagaki, N. Li, K. Svoboda, S. Druckmann, An orderly single-trial
1384 organization of population dynamics in premotor cortex predicts behavioral
1385 variability. *Nat Commun* **10**, 216 (2019).
1386 57. Z. Wei, B. J. Lin, T. W. Chen, K. Daie, K. Svoboda, S. Druckmann, A comparison of
1387 neuronal population dynamics measured with calcium imaging and
1388 electrophysiology. *PLoS Comput Biol* **16**, e1008198 (2020).
1389 58. B. Haimson, O. D. Gilday, A. Lavi-Rudel, H. Sagi, E. Lottem, A. Mizrahi, Single neuron
1390 responses to perceptual difficulty in the mouse auditory cortex. *Sci Adv* **10**,
1391 eadp9816 (2024).
1392 59. A. E. Takesian, V. C. Kotak, D. H. Sanes, Age-dependent effect of hearing loss on
1393 cortical inhibitory synapse function. *J Neurophysiol* **107**, 937-947 (2012).
1394 60. A. E. Takesian, V. C. Kotak, D. H. Sanes, Presynaptic GABA(B) receptors regulate
1395 experience-dependent development of inhibitory short-term plasticity. *J Neurosci*
1396 **30**, 2716-2727 (2010).
1397 61. A. Gilad, I. Maor, A. Mizrahi, Learning-related population dynamics in the auditory
1398 thalamus. *Elife* **9**, e56307 (2020).

62. O. D. Gilday, B. Praegel, I. Maor, T. Cohen, I. Nelken, A. Mizrahi, Surround suppression in mouse auditory cortex underlies auditory edge detection. *PLoS Comput Biol* **19**, e1010861 (2023).
63. H. Shani-Narkiss, A. Vinograd, I. D. Landau, G. Tasaka, N. Yayon, S. Terletsky, M. Groysman, I. Maor, H. Sompolinsky, A. Mizrahi, Young adult-born neurons improve odor coding by mitral cells. *Nat Commun* **11**, 5867 (2020).
64. O. D. Gilday, A. Mizrahi, Learning-Induced Odor Modulation of Neuronal Activity in Auditory Cortex. *J Neurosci* **43**, 1375-1386 (2023).
65. J. J. Jun, N. A. Steinmetz, J. H. Siegle, D. J. Denman, M. Bauza, B. Barbarits, A. K. Lee, C. A. Anastassiou, A. Andrei, C. Aydin, M. Barbic, T. J. Blanche, V. Bonin, J. Couto, B. Dutta, S. L. Gratiy, D. A. Gutnisky, M. Hausser, B. Karsh, P. Ledochowitsch, C. M. Lopez, C. Mitelut, S. Musa, M. Okun, M. Pachitariu, J. Putzeys, P. D. Rich, C. Rossant, W. L. Sun, K. Svoboda, M. Carandini, K. D. Harris, C. Koch, J. O'Keefe, T. D. Harris, Fully integrated silicon probes for high-density recording of neural activity. *Nature* **551**, 232-236 (2017).
66. M. Pachitariu, N. Steinmetz, S. Kadir, M. Carandini, H. Kenneth D, Kilosort: realtime spike-sorting for extracellular electrophysiology with hundreds of channels. *bioRxiv*, 061481 (2016).
67. P. Shamash, M. Carandini, K. Harris, N. Steinmetz, A tool for analyzing electrode tracks from slice histology. *BioRxiv*, 447995 (2018).
68. W. E. Vinje, J. L. Gallant, Sparse coding and decorrelation in primary visual cortex during natural vision. *Science* **287**, 1273-1276 (2000).
69. D. M. Green, J. A. Swets, *Signal detection theory and psychophysics* (Wiley New York, 1966), vol. 1.

1424

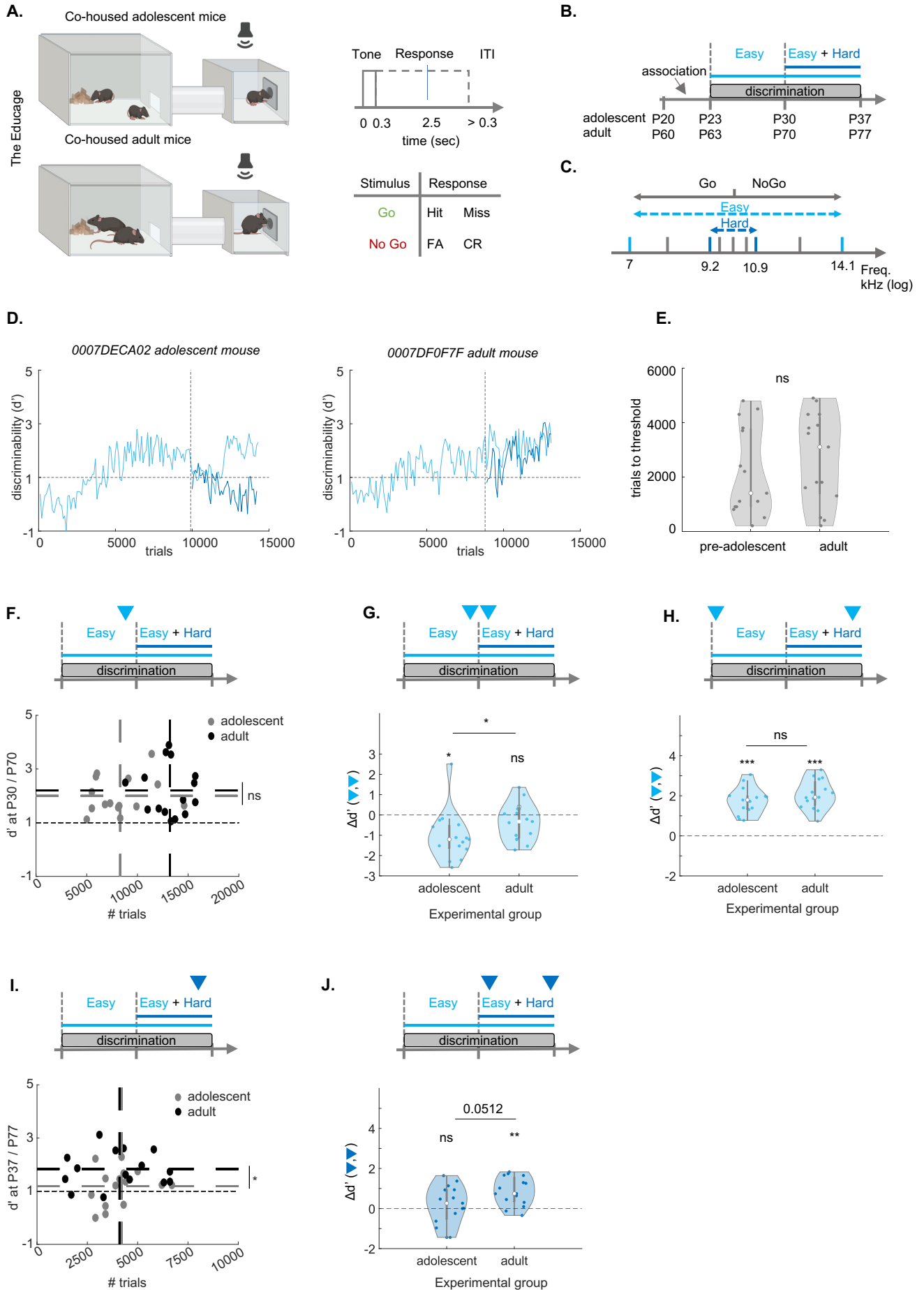
A.
Co-housed adolescent mice
The Educage
Co-housed adult mice
Tone
Response
ITI
0 0.3
2.5
> 0.3
time (sec)
Stimulus
Response
Go
Hit
Miss
No Go
FA
CR
B.
Easy
Easy + Hard
association
discrimination
adolescent
adult
P20
P60
P23
P63
P30
P70
P37
P77
C.
Go
NoGo
Easy
Hard
7
9.2
10.9
14.1
Freq.
kHz (log)
D.
0007DECA02 adolescent mouse
0007DF0F7F adult mouse
discriminability (d')
trials
E.
ns
trials to threshold
pre-adolescent
adult
F.
Easy
Easy + Hard
discrimination
adolescent
adult
d' at P30 / P70
ns
trials
G.
Easy
Easy + Hard
discrimination
*
ns
Δd' (▼,▼)
adolescent
adult
Experimental group
H.
Easy
Easy + Hard
discrimination
ns
***
***
Δd' (▼,▼)
adolescent
adult
Experimental group
I.
Easy
Easy + Hard
discrimination
adolescent
adult
d' at P37 / P77
*
trials
J.
Easy
Easy + Hard
discrimination
0.0512
ns
**
Δd' (▼,▼)
adolescent
adult
Experimental group

Fixed effects	Estimate	SEM	T-statistic	DF	P-value**	CI (lower)	CI (upper)
Intercept	1.6001	0.2312	6.9222	27	3.8798e-07	1.1258	2.0744
Age	0.5994	0.2266	2.6457	27	0.0269	0.1346	1.0643
Sex	-0.0428	0.2476	-0.1729	27	0.9999	-0.5509	0.4653

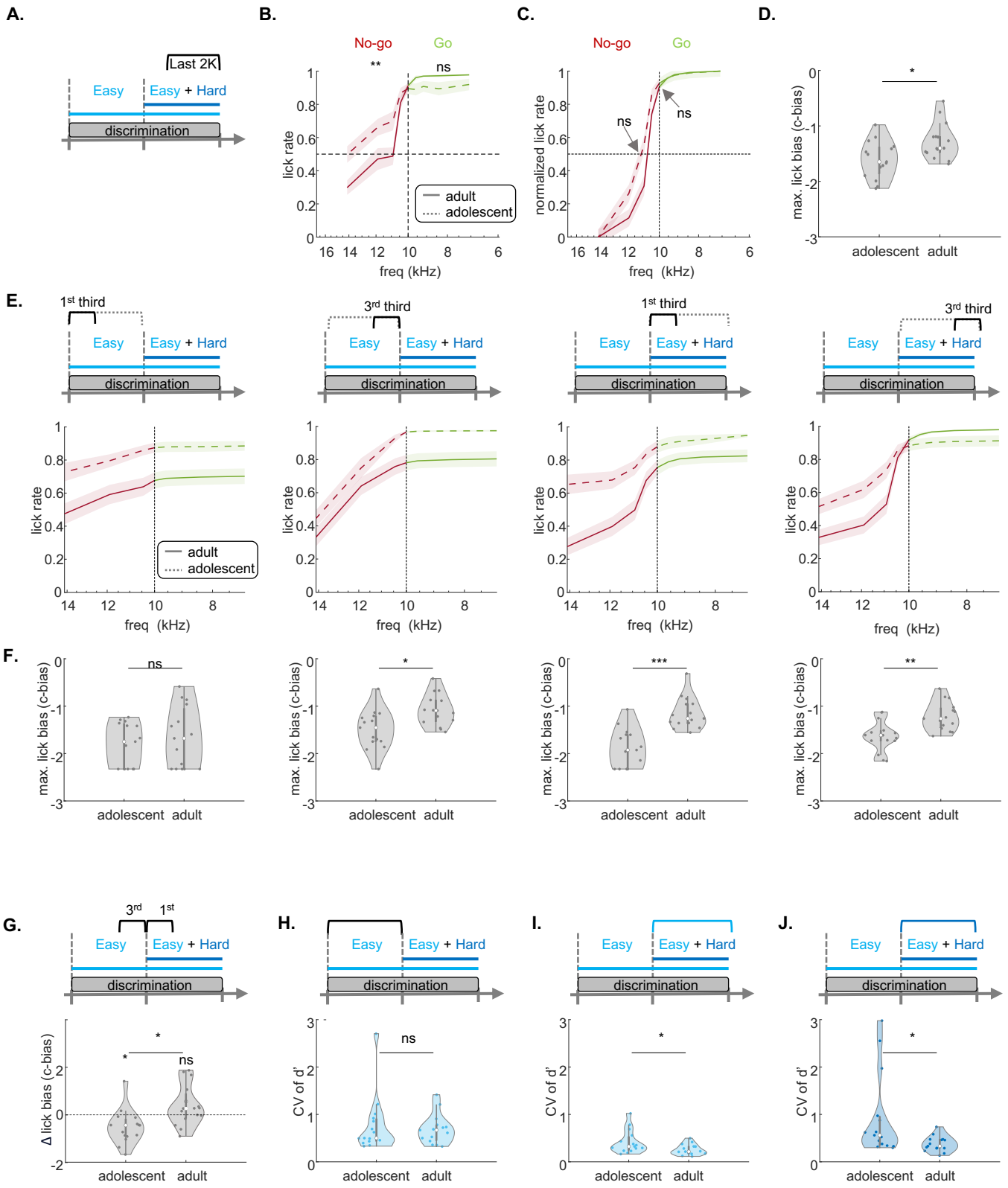
A.
Last 2K
Easy
Easy + Hard
discrimination
B.
No-go
Go
**
ns
lick rate
adult
adolescent
freq (kHz)
C.
No-go
Go
ns
ns
normalized lick rate
freq (kHz)
D.
*
max. lick bias (c-bias)
adolescent
adult
E.
1st third
3rd third
1st third
3rd third
Easy
Easy + Hard
discrimination
lick rate
adult
adolescent
freq (kHz)
F.
ns
*
***
**
max. lick bias (c-bias)
adolescent
adult
G.
3rd
1st
Easy
Easy + Hard
discrimination
*
*
ns
Δ lick bias (c-bias)
adolescent
adult
H.
ns
CV of d'
I.
*
CV of d'
J.
*
CV of d'

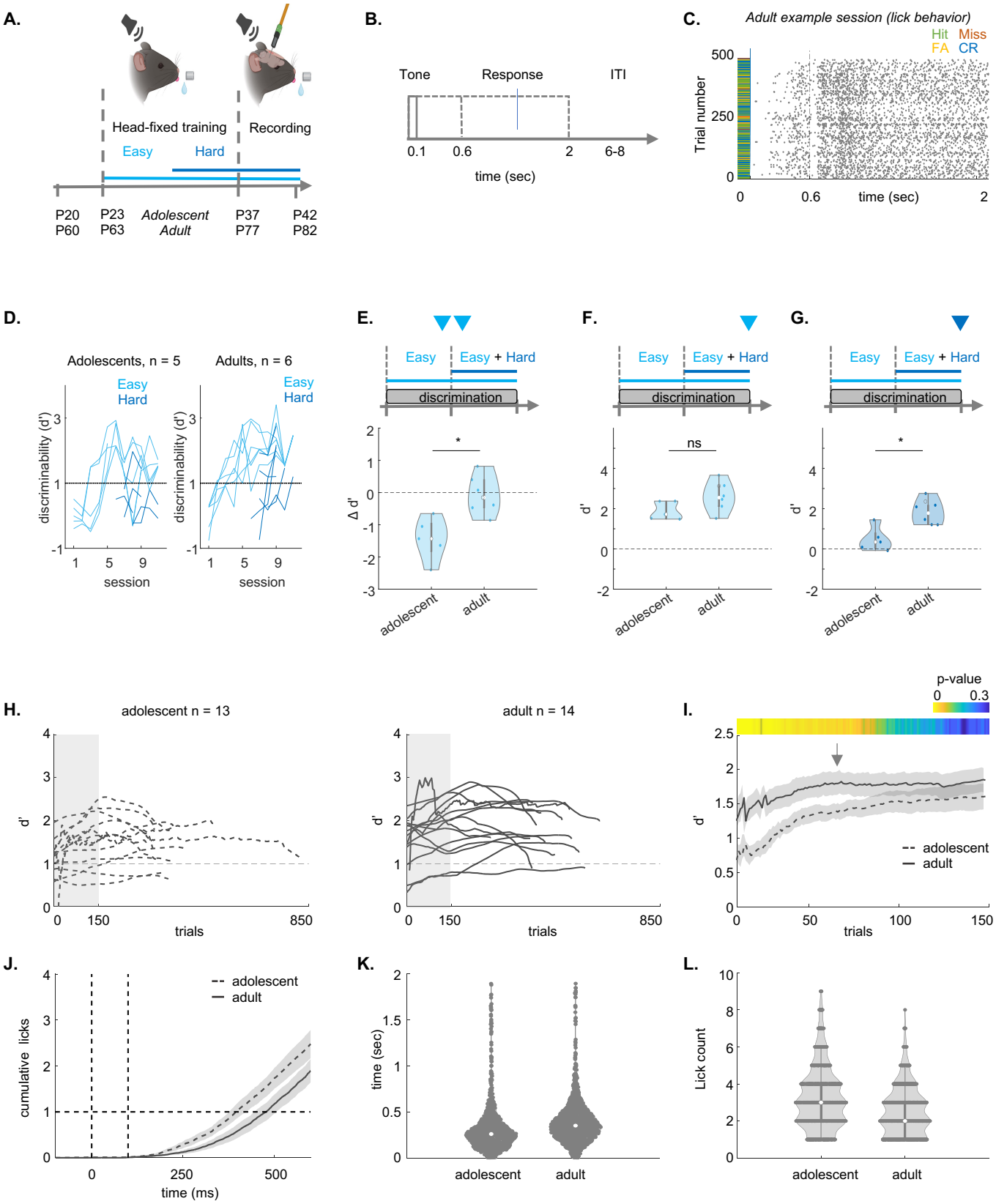
A.
Head-fixed training
Recording
Easy
Hard
P20
P60
P23
P63
Adolescent
Adult
P37
P77
P42
P82
B.
Tone
Response
ITI
0.1
0.6
2
6-8
time (sec)
C.
Adult example session (lick behavior)
Hit
Miss
FA
CR
Trial number
500
250
0
0
0.6
time (sec)
2
D.
Adolescents, n = 5
Adults, n = 6
Easy
Hard
discriminability (d')
session
E.
Easy
Easy + Hard
discrimination
Δ d'
*
adolescent
adult
F.
ns
d'
G.
H.
adolescent n = 13
adult n = 14
trials
I.
p-value
0
0.3
adolescent
adult
J.
cumulative licks
time (ms)
K.
time (sec)
L.
Lick count

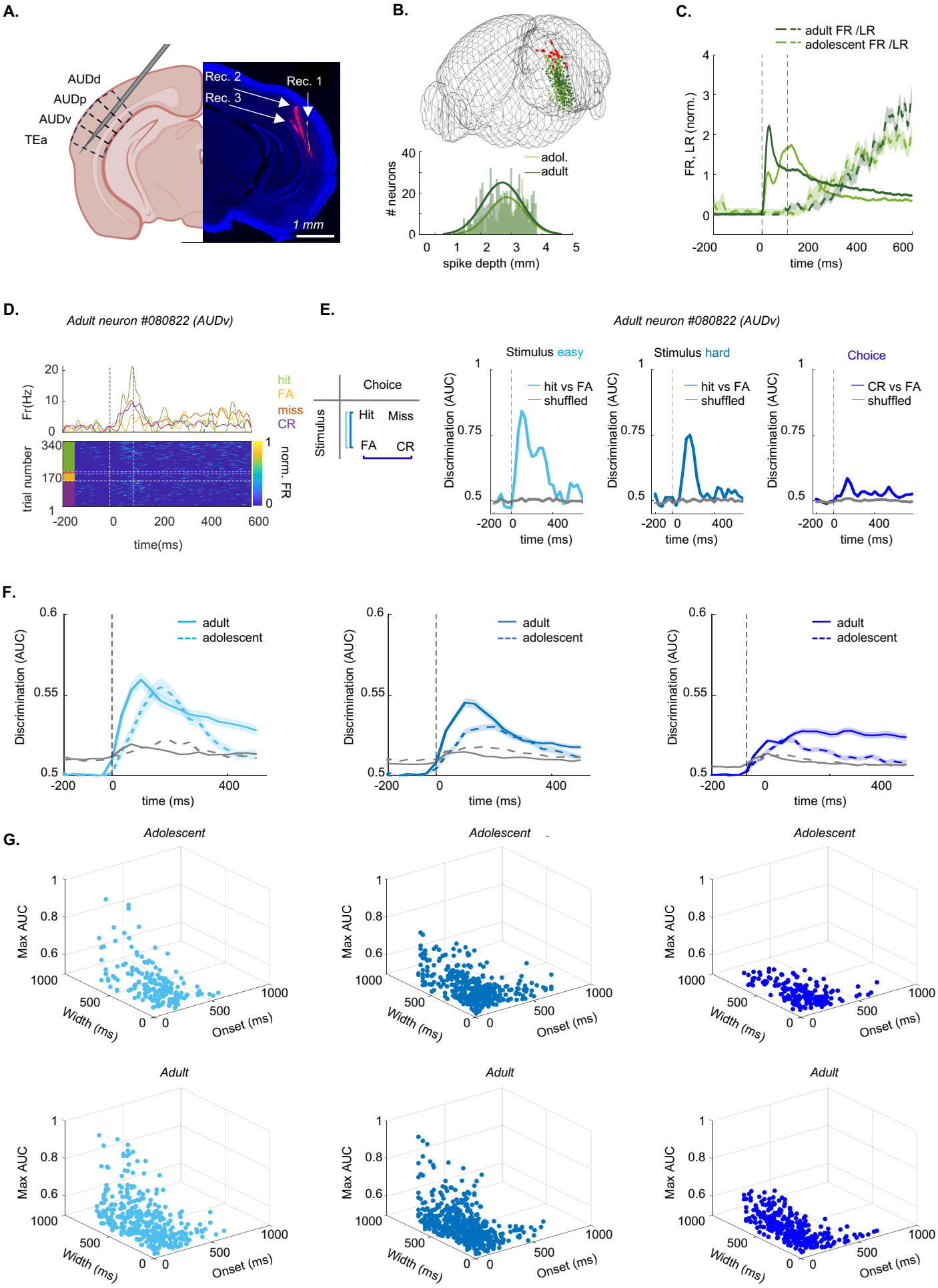
A.
AUDd
AUDp
AUDv
TEa
Rec. 2
Rec. 1
Rec. 3
1 mm
B.
adol.
adult
neurons
spike depth (mm)
C.
adult FR /LR
adolescent FR /LR
FR, LR (norm.)
time (ms)
D.
Adult neuron #080822 (AUDv)
Fr(Hz)
hit
FA
miss
CR
trial number
norm. FR
time(ms)
E.
Adult neuron #080822 (AUDv)
Choice
Stimulus
Hit
Miss
FA
CR
Stimulus easy
Stimulus hard
Choice
hit vs FA
shuffled
CR vs FA
Discrimination (AUC)
time (ms)
F.
adult
adolescent
Discrimination (AUC)
time (ms)
G.
Adolescent
Adult
Max AUC
Width (ms)
Onset (ms)

Stimulus easy							
Fixed Effects	Estimate	StandardError	tStatistic	DF	pValue	CI lower	CI upper
Intercept	163.6104	7.9457	20.591	522	6.29587E-69	148.0009	179.2199
Onset (ms)	-29.7978	9.7626	-3.0523	522	0.00716101	-48.9765	-10.6191
Intercept	216.2921	13.2858	16.2799	522	5.15393E-48	190.1919	242.3924
Duration (ms)	63.2599	16.3499	3.8691	522	0.000369146	31.1401	95.3796
Intercept	0.6035	0.007	85.6404	522	0.0001	0.5897	0.6174
Max AUC	0.0172	0.0087	1.9776	522	0.145507056	0.0001	0.0342
Stimulus hard							
Fixed Effects	Estimate	StandardError	tStatistic	DF	pValue	CI lower	CI upper
Intercept	151.1905	5.4684	27.6479	941	3.6685E-123	140.4588	161.9222
Onset (ms)	-35.3357	7.1998	-4.9079	941	3.25392E-06	-49.4651	-21.2063
Intercept	220.614	8.4357	26.1525	941	2.8344E-113	204.0591	237.1689
Duration (ms)	55.6268	11.1065	5.0085	941	1.9647E-06	33.8305	77.4231
Intercept	0.5821	0.0034	170.2777	941	0.0001	0.5754	0.5888
Max AUC	0.0098	0.0045	2.1862	941	0.087143965	0.001	0.0187
Choice							
Fixed Effects	Estimate	StandardError	tStatistic	DF	pValue	CI lower	CI upper
Intercept	174.5856	8.259	21.139	518	1.6732E-71	158.3605	190.8108
Onset (ms)	-24.3644	10.2288	-2.3819	518	0.052746707	-44.4595	-4.2693
Intercept	228.1768	12.92	17.6607	518	1.64628E-54	202.7947	253.5589
Duration (ms)	82.0002	16.0017	5.1245	518	1.26556E-06	50.564	113.4363
Intercept	0.5491	0.0027	200.1358	518	0.0001	0.5437	0.5545
Max AUC	0.0166	0.0034	4.8959	518	3.92843E-06	0.01	0.0233

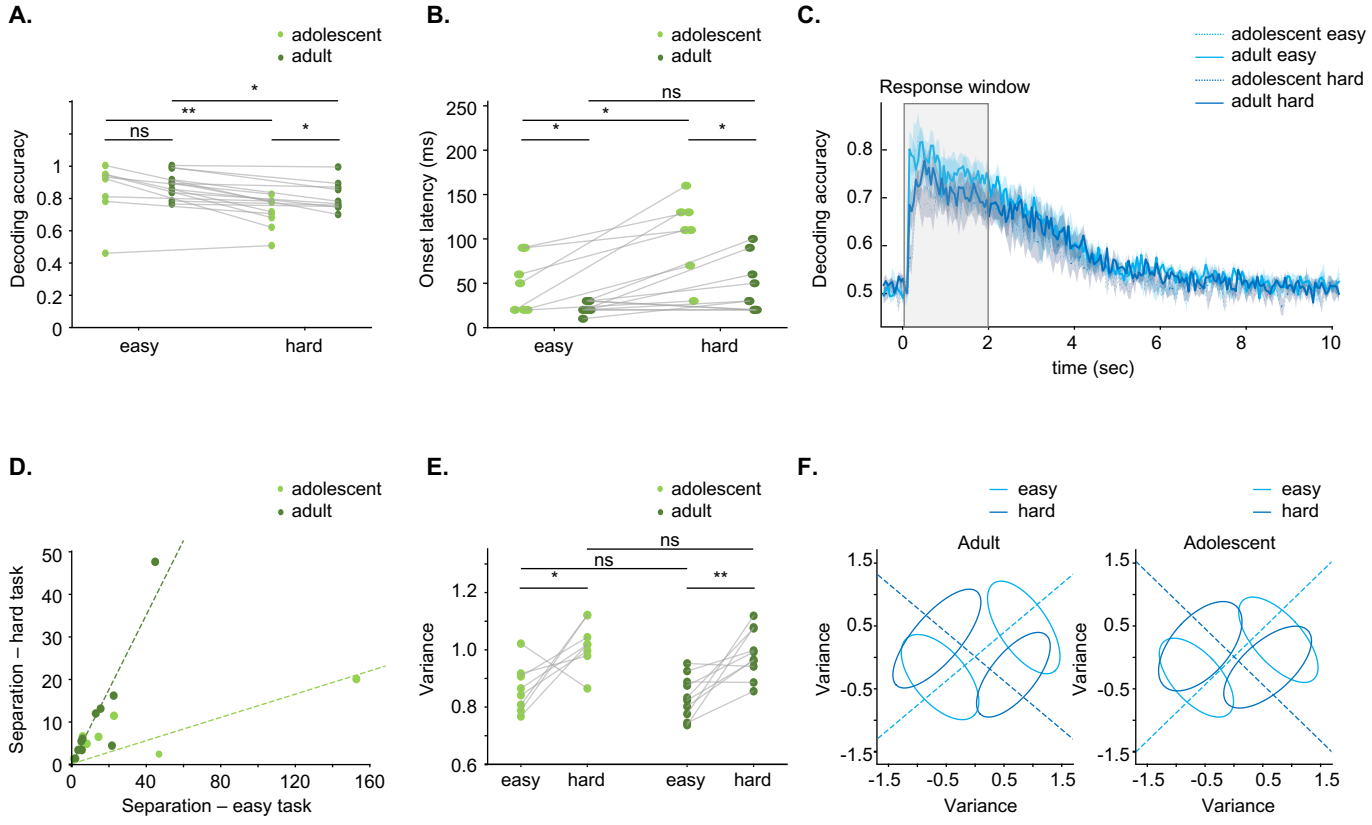
A.
adolescent
adult
Decoding accuracy
ns
**
*
*
easy
hard
B.
adolescent
adult
Onset latency (ms)
ns
*
*
*
easy
hard
C.
adolescent easy
adult easy
adolescent hard
adult hard
Response window
Decoding accuracy
time (sec)
D.
adolescent
adult
Separation – hard task
Separation – easy task
E.
adolescent
adult
Variance
ns
ns
*
**
easy
hard
easy
hard
F.
easy
hard
Adult
Adolescent
Variance
Variance

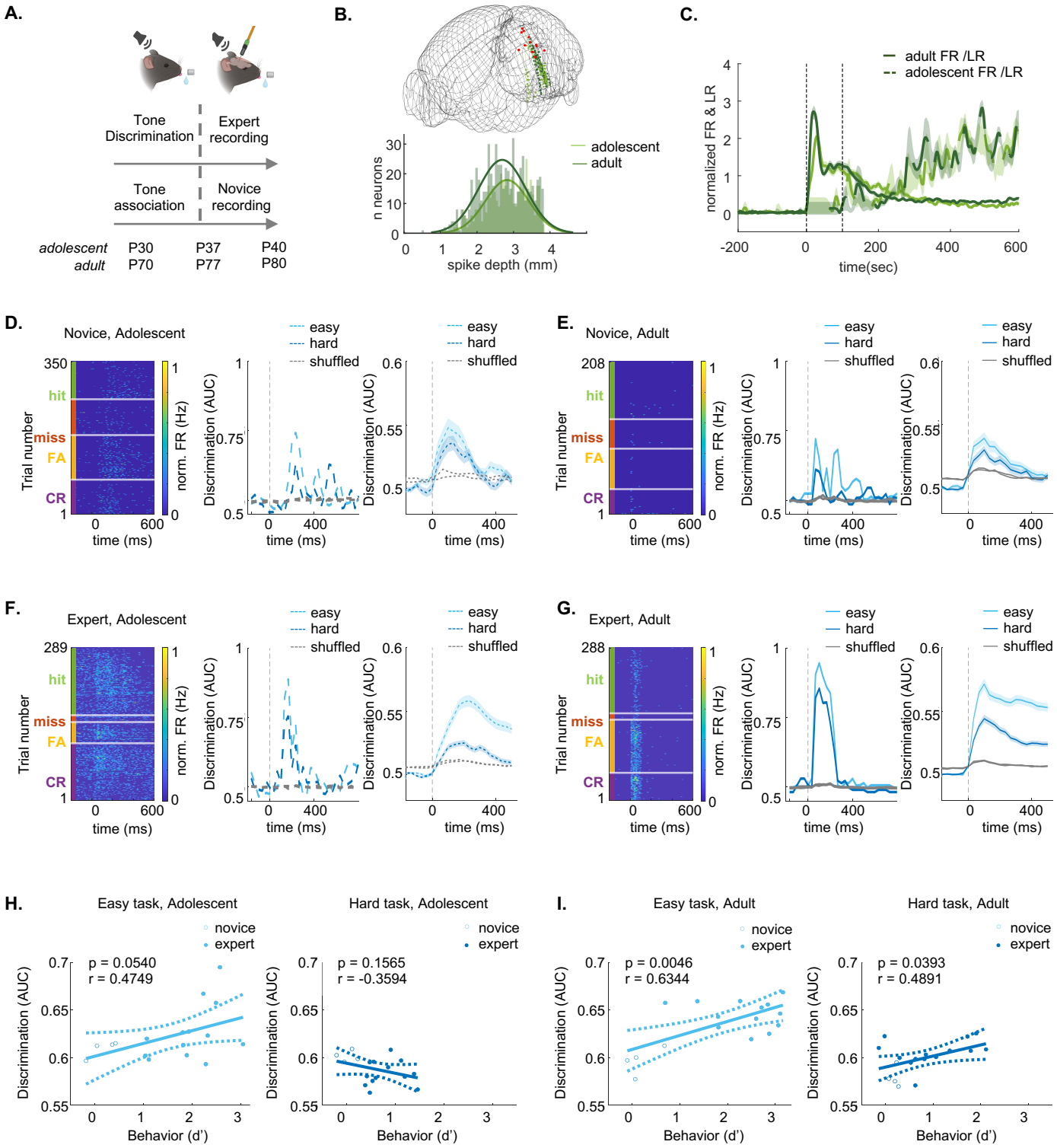
A.
Tone Discrimination
Expert recording
Tone association
Novice recording
adolescent P30 P37 P40
adult P70 P77 P80
B.
n neurons
spike depth (mm)
adolescent
adult
C.
adult FR /LR
adolescent FR /LR
normalized FR & LR
time(sec)
D.
Novice, Adolescent
Trial number
hit
miss
FA
CR
norm. FR (Hz)
time (ms)
Discrimination (AUC)
easy
hard
shuffled
E.
Novice, Adult
F.
Expert, Adolescent
G.
Expert, Adult
H.
Easy task, Adolescent
Hard task, Adolescent
novice
expert
p = 0.0540
r = 0.4749
p = 0.1565
r = -0.3594
Behavior (d')
I.
Easy task, Adult
Hard task, Adult
p = 0.0046
r = 0.6344
p = 0.0393
r = 0.4891

Fixed Effects Onset Latency(ms)	Estimate	SEM	T-Statistic	DF	P-Value	CI lower	CI upper
Intercept	92.6519	3.8909	23.8125	2582	5.4024E-113	85.0223	100.2815
Age	-22.6378	5.0624	-4.4718	2582	2.42782E-05	-32.5645	-12.7111
Learning	5.6206	8.7235	0.6443	2582	0.9999	-11.4851	22.7263
Task difficulty	0.8813	5.4571	0.1615	2582	0.9999	-9.8194	11.5819
Age- Learning	-6.8831	11.1114	-0.6195	2582	0.9999	-28.6713	14.905
Age - Difficulty	0.2461	7.2185	0.0341	2582	0.9999	-13.9085	14.4006
Learning - Difficulty	-2.5145	12.3257	-0.204	2582	0.9999	-26.6837	21.6546
Age-Learning-Difficulty	4.4526	15.7691	0.2824	2582	0.9999	-26.4688	35.374

Fixed Effects Duration of Discrimination (ms)	Estimate	SEM	T-Statistic	DF	P-Value	CI lower	CI upper
Intercept	299.7098	7.8305	38.2747	2582	8.4469E-254	284.3551	315.0645
Age	63.2136	9.2513	6.833	2582	3.1017E-11	45.0729	81.3544
Learning	-88.8699	15.9421	-5.5745	2582	8.21813E-08	-120.1306	-57.6092
Task difficulty	-53.9606	9.9745	-5.4098	2582	2.06623E-07	-73.5194	-34.4017
Age- Learning	-30.6998	20.3155	-1.5112	2582	0.3926	-70.5361	9.1365
Age - Difficulty	-18.8772	13.194	-1.4307	2582	0.4579	-44.749	6.9947
Learning - Difficulty	53.8178	22.5289	2.3888	2582	0.0509	9.6414	97.9943
Age-Learning-Difficulty	12.9698	28.823	0.45	2582	0.9999	-43.5488	69.4884

Fixed Effects Maximal Discrimination (AUC)	Estimate	SEM	T-Statistic	DF	P-Value	CI lower	CI upper
Intercept	0.6278	0.0042	148.636	2582	0.0001	0.6195	0.6361
Age	0.024	0.0056	4.2953	2582	5.42797E-05	0.0131	0.035
Learning	-0.0249	0.0096	-2.5859	2582	0.029303232	-0.0438	-0.006
Task difficulty	-0.0438	0.006	-7.24	2582	1.76807E-12	-0.0556	-0.0319
Age- Learning	-0.03	0.0123	-2.4376	2582	0.0446	-0.0541	-0.0059
Age - Difficulty	-0.0023	0.008	-0.2846	2582	0.9999	-0.0179	0.0134
Learning - Difficulty	0.0394	0.0136	2.8893	2582	0.0116	0.0127	0.0662
Age-Learning-Difficulty	-0.0094	0.0175	-0.5387	2582	0.9999	-0.0437	0.0248

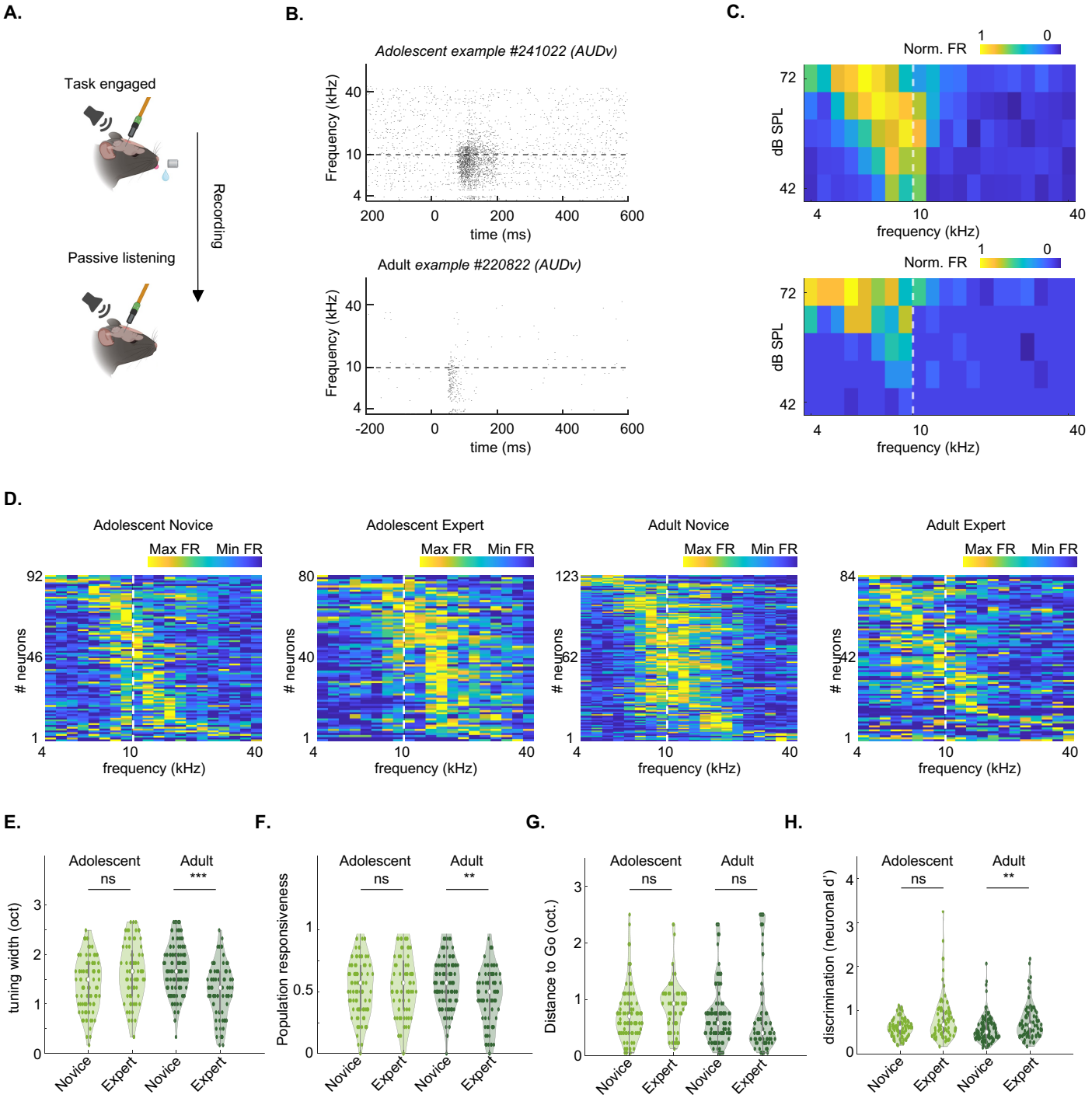
A.
Task engaged
Recording
Passive listening
B.
Adolescent example #241022 (AUDv)
Frequency (kHz)
time (ms)
Adult example #220822 (AUDv)
C.
Norm. FR
dB SPL
frequency (kHz)
D.
Adolescent Novice
Adolescent Expert
Adult Novice
Adult Expert
Max FR
Min FR
neurons
frequency (kHz)
E.
tuning width (oct)
F.
Population responsiveness
G.
Distance to Go (oct.)
H.
discrimination (neuronal d')
Adolescent
Adult
ns
***
**
Novice
Expert